Recent advances on the recognition of the explosive Mother of Satan: A review

Priyanka Sharma[a], Mainak Ganguly*[a], Ankita Doi[a] and Mamta Sahu[a]

[a]Department of Chemistry, Manipal University Jaipur, Jaipur-Ajmer Express Highway, Dehmi Kalan, Jaipur, Rajasthan 303007, India

Email: **mainak.ganguly@jaipur.manipal.edu**

Abstract

Due to the ease of synthesis and use, improvised explosive devices pose a significant global security threat. Triacetone triperoxide (TATP) is a commonly used peroxide-based explosive with a detonation strength reported to be about 88% higher than that of trinitrotoluene (TNT). Detection of TATP at security-sensitive locations such as airports and railway stations is particularly challenging because its molecular structure lacks nitrogen-containing functional groups (e.g., $N–NO_2$ or N–N bonds) typically targeted by conventional explosive detection systems. In addition, TATP readily sublimes at room temperature and, unlike most nitro-explosives, leaves minimal or no detectable post-blast residues.

In certain analytical assays, TATP can generate products like hydrogen peroxide (H_2O_2) when chromogenic reagents such as titanyl oxalate are used in microfluidic paper-based devices, although the color intensity is significantly weaker. Various technical type detection approaches have been reported, including trained animals, spectroscopic techniques, electrical conductivity-based gas sensing, fluorogenic detection (quenching- or enhancement-based), colorimetric assays etc. Recent studies also have highlighted nanomaterial-assisted sensing strategies, including nanoparticle and nanocluster-based detection employing current variation, fluorescence alteration and color change. Spot analysis was also documented in this aspect.

Keywords: Explosive; mass killing; advanced sensing technology; antiterrorism; Nanotechnology.

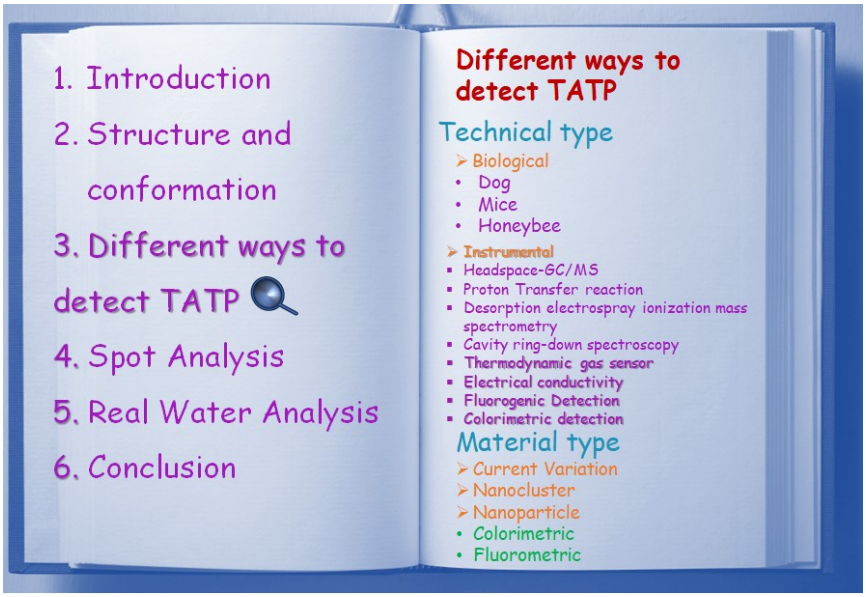

Different modes of detection of the triacetone triperoxide.

.

1. Introduction

Explosive detection is a crucial issue in homeland security and counterterrorism. Due to the simplicity of production and usage, explosive bombs have been the most prevalent kind of terrorism, killing tens of thousands of people along with immense property damage.[1] The current increase in international terrorism, linked to mass killing, has prompted the need for standoff/remote, sensitive, and affordable explosive detection. Because of the extensive usage of explosive formulas, the study of explosives has also been critical in forensic research, land-mine sensing, ecological challenges, and explosive residues.[2] Based on their structural characteristics, the 229 explosive compounds listed by the Bureau of Alcohol, Tobacco, and Firearms (ATF) through November 2010 can be broadly categorized into six groups. Nitro aromatics (NACs), like TNT and 2,4-dinitrotoluene (2,4-DNT), are often the main explosive used in military operations as well as the main ingredients in unexploded landmines all over the world.[3] The primary ingredients of extremely powerful plastic explosives like C-4 (91 %- Royal Demolition Explosive) and Semtex (40 to 76 % percent- pentaerythritol tetranitrate) are nitroperhydro-1,3,5-triazine (RDX) and 3,5-trinitroperhydro-1,3,5-triazine (PETN). Solid rocket propellants frequently contain ammonium salts like ammonium-nitrate and ammonium-phosphate, which were frequently utilized in industrial applications.[4] Due to their ease of synthesis from cheap components, peroxide-based explosives like triacetone triperoxide (TATP) and hexamethylene triperoxide diamine (HMTD) have become more popular among homemade explosives. Most extremely powerful explosives are nitro-substituted (nitrated) substances. Wolffenstein discovered and synthesized triacetone triperoxide (TATP) in the 19th century.[5] TATP is extremely sensitive to an explosion with mere boiling or friction, earning the nickname "Triacetone peroxide".[6] TATP is both sublime & volatile, making it unsuitable for soldierly or technical applications. This home-made explosive is widely utilized in terrorist acts due to its tremendous explosion force and simple synthesis.[7, 8] However, it has primarily been cast off in terrorist actions because it can be easily made from house-hold chemicals ($(CH_3)_2O$, H_2O_2, and battery acid), readily available from hardware supplies and cosmetics stores.[9] It was used in several terror efforts, including the 2005 London Subway[10] explosion, an unsuccessful terrorist attempt on a Northwest Airlines aeronautical in 2009, the Paris-suicide bombing in 2015, the Brussels Airport attack in 2016, and the Manchester-concert bombing in 2017.[11] Home-made TATP participated in terrorist activities in the USA, Israel, or, more recently, the assaults on May 16 in Casablanca, Morocco.

TATP detection by regular test methods at public protection-regulated hotspots (like train and airline terminals) is problematic, since its chemical structure lacks an N- group or another instrumentally sensitive functional group. TATP has a sugar-like look, but it does not absorb or emit light in the relevant UV range of the electromagnetic spectrum.[12, 13] TATP quickly sublimes at room temperature and, unlike conventional nitro-explosives, TATP does not leave post-blast residues. TATP may produce

similar colored products to H_2O_2 when chromogenic reagents (such as titanyl oxalate) are used on microfluidic paper-based analytical devices, albeit at a considerably lower color intensity.[14] It is made by reacting acetone with hydrogen peroxide and sulfuric acid. This reaction's predominant product is trimer peroxide I, which melts at 98.8 °C. Additionally, dimer peroxide II, which melts at 132.8 °C, is the minor product. Both of their crystalline forms can burst violently with sudden, intense heating, shock, rubbing, or electrostatic discharge (especially when dry). They are both soluble in acetone but insoluble in water.

TATP does not glow and does not absorb much light in the UV area. As a result, infrared and Raman spectroscopy, enzyme-based assays, and mass spectrometry (MS) have been used mainly to identify them.[15-18] Each of these techniques has significant flaws, including limited sensitivity and/or sluggish reaction. This nine-membered cyclic peroxide-based explosive is characterized by its great sensitivity to an explosion on heating, impact, or friction.[19-23]

2. Conformation and Structure of TATP

Dubnikova and colleagues[24] investigated the construction and configuration of free TATP molecules as well as seven TATP ion complexes. TATP is a home-made explosive that can avoid exposure via usual cast-off sensors. Researchers employed quantum chemical methods to calculate the conformation and bond strength among TATP or various ions. The strongest bonds were observed among the ions tested between TATP and zinc(II) and indium (III), indicating their superior affinity. The interactions with antimony (III), scandium (III), and titanium (IV) led to the cleavage of the TATP ring. In the complex tested, TATP molecules and indium (III) ions had the maximum binding energy. Notably, the TATP-Zn^{2+} complex displayed over 23 kcal/mol higher energy favourability compared to the TATP-Cd^{2+} complex. In terms of monovalent ions, the composite formed with lithium(I) was preferred over the composite with copper (I), based on the energetics of the interactions. The research does not provide a thorough explanation of the intricate interaction process between TATP and the sensing/recognition units, instead concentrating on the detection performance and ion–TATP complex formation. The conversion of molecular recognition into quantifiable optical or electrical signals in sensing devices is not systematically discussed. Additionally, it offers little details on coordination interaction, charge transfer, and signal transduction pathways that oversee detection. Moreover, the effect of nanomaterials in improving sensitivity, surface contact, fluorescence amplification, or catalytic sensing performance is not covered. Instead of using portable experimental sensing instruments, the study mostly uses theoretical and laboratory-based computations. It is not evaluated in real-world settings with complicated sample matrices, humidity, and interfering vapors. Furthermore, sensor stability, repeatability, reaction time, and long-term operating performance all crucial for practical field detection of TATP are not covered by the technique.

Method of calculation

Molecular mechanics force field calculations (specifically MMFF94) were conducted using the SPARTAN code (specifically Spartan SGI, version 5.1.3 OpenGL) to generate an estimate of a consistent primary geometry & determine the greatest steady configuration of TATP, as well as specific ion TATP complexes. The lowest energy geometry of the Zn^{2+} complex with TATP was thoroughly explored using the molecular mechanics code. Geometry optimization was undertaken using several starting configurations to acquire the utmost steady conformation. Additionally, calculations were carried out for TATP complexes with several ions. The Hartree-Fock method was utilized with a 3-21G basis set for the H, C, and O atoms, along with a Hay-Wadt LANL2DZ effective core potential (ECP) for all ions.[24]

A comparison of the molecular conformation of the nonagonal ring in both structures indicates that the bond lengths and angles do not differ considerably from one another and are almost identical to those found in the crystal structure of the unsolved TATP. The molecules of methanol that make up TATP (TATP.methanol) were disorganized over six different locations. Although twelve configurations were conceivable from a crystallographic point of view, only six of these positions could be achieved. Each of these six orientations allows for a hydrogen bond to be formed with the oxygen ring atoms. A close packing arrangement in the shape of a hexagon in these columns. In contrast to the density of unsolved TATP (1.272 g cm^{-3}), the density of the crystal structure of TATP.methanol was obtained to be 1.090 g cm^{-3}, which was a lesser value due to the voids inside the crystal structure [Fig. 1].[25, 26] The molecular interaction mechanism between TATP and sensing/recognition systems, it focuses primarily on the behavioral performance and selection efficiency of dogs for explosive detection. The concepts of signal conversion used in analytical detection techniques. The study primarily relies on the behavioral reactions of the animals, which might change because of human influence, ambient factors, exhaustion, and training quality. Its sensitivity and repeatability are not thoroughly compared to those of contemporary instrumental or nanomaterial-based sensing systems. The approach may also encounter difficulties with large-scale field deployment, quantitative analysis, and continuous real-time monitoring. The molecular recognition process between TATP and antibodies and the principles of signal transduction in sensing systems are not comprehensively explained by the manufacture of TATP haptens and antibody-based detection performance. Interaction routes including hydrogen bonding, immunological recognition, and charge-transfer processes that are involved in detection are not thoroughly discussed. Moreover, little research has been done on nanomaterials might improve signal amplification, sensitivity, and selectivity. Practical drawbacks of the testing approach include its reliance on controlled laboratory settings, potential instability of antibodies, limited long-term repeatability, and difficulties with real-time field analysis of TATP vapor.

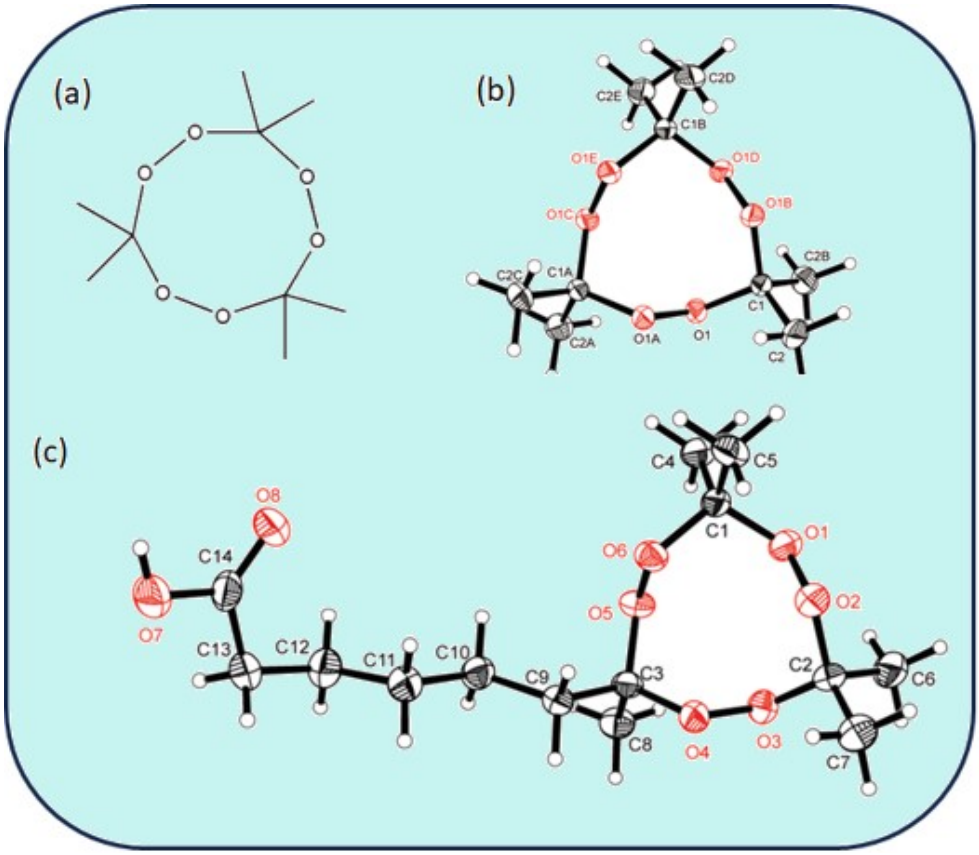

Fig. 1: (a) Structure of TATP (b) Conformation and atomic numbering of TATP (c) TATP hapten conformation and atomic numbering (reprinted with permission Walter et al.[26]).

3. Different ways to detect TATP

Table 1: Analytical parameters (LOD, LOQ) for technical type

Technical type	*LOD*	*LOQ*	*Linear range*
With animals[26]	*65µg L*$^{-1}$	-	-
Headspace Gas Chromatography–Mass Spectrometry method [41]	*0.1 ng*	-	-
Proton transfer reaction[27]	*1.3 ppb*	-	-
Thermodynamic based gas sensors[28]	*8 ppm*	-	*~ 3.5 ppm*
Electrochemical detection • *Organic-semiconductor sensors*[29] • *With molecular imprinted polymer*[35]	*100 ppb* *26.9 µg·L*$^{-1}$	- *81.6 µg·L*$^{-1}$ -	- - -

• *glassy-carbon electrode* [36]	*50 ng*		
Fluorogenic detection of TATP • *Enhancement-based detection*[30] • *2,4-diuorophenyl or 4-trifluoromethylphenyl*[31] • *fluorenyl boronate ester*[32] • *pro chelator/Zn^{2+}*[33]	*0.1 mg*	-	*100 nmol*
	2.5 ppb	-	-
	40 ppb	-	*5.3 ppm*
	10nm	-	*10 µM- 10nm*
Colorimetric detection of TATP[34]	*20 µg/mL*	-	-

Table 2: Analytical parameters (LOD, LOQ) for material type

Material type	*LOD*	*LOQ*	*Linear range*
Gold nanoclusters cross-link polyphenylenevinylene[37]	*50 ppb*	-	*550 to 50 ppb*
Polyaniline[38]	*15 ppm*	-	*1-100 ppm*
Gold nanoparticles[39]	*15 µg L^{-1}*	-	*0.1- 1mg L^{-1}*
3-Aminopropyl triethoxysilane@ titanium di oxide nanoparticle[40]	*5.13× 10^{-4} mol/L*	-	-
TATP-Fe^{2+}- tetramethylbenzidine[41]	*0.12 µM*	-	*0.5–30 µM*
Silver Nanoparticles[42]	*0.31 mg L^{-1}*	-	*1.25–31.25 mg L^{-1}*
Fe_3O_4 Magnetic Nanoparticles on Nafion[43]	*0.47 mg/L*	*1.57 mg/L*	*10 mg L^{-1}*

Silver Nanoparticles incorporated into a Zinc-based Metal-Organic Framework (Ag@ZnMOF) composite[44]	*0.10 mg L^{-1}*	-	-
Goethite nanoparticles[72]	*3.3 mg L^{-1}*	*10.8 mg L^{-1}*	-
Turn on-off-on" sensing with Hg^{2+} and TATP[73]	*0.055 mg L^{-1}*	-	*2.5 to 50 mg L^{-1}*
Silica nanoparticle[45]	*620 µM*	-	*0.2 mg L^{-1}*
Ascorbic acid-Polyethyleneimine-Triethylenetetramine Carbon quantum Dots[79]	*0.18 nmol l^{-1}*		
Ascorbic acid-urea-carbon dots[80]	*3.0 nmol L^{-1}*		

3.1 Technical type

3.1.1. *With Animals*

People widely utilize dogs for various purposes, including detecting explosives, drugs, biological threats, disease biomarkers, and rescue missions for missing individuals.[26] Triacetone triperoxide serves as a cost-effective alternative to explosives like TNT highlighting the pressing need for effective TATP detection methods. Walter and colleagues[26] established a TATP analogue to produce an immunogen for generating antibodies in two immunized mice. The LOD for TATP was 65 µg/L^{-1} and 870 ng/mL, respectively, in an enzyme-linked immunosorbent test (ELISA) utilizing sera from immunized mice. [46, 47] The testing method's actual application in real-time field detection is limited by its primary reliance on controlled laboratory settings. Concerns including long-term operating performance, environmental interference, repeatability, and antibody stability were not thoroughly assessed.

Onodea and colleagues[48] thoroughly examined a security and safety device known as an "electric-canine nose." That device relies on a plasmon resonance at the surface (SPR) sensor and the interaction between antigens & antibodies. The primary focus of their study was to develop sensor surfaces that are well-suited for practical applications of the SPR sensor. Furthermore, they demonstrated the

development of techniques for sampling explosives or presented a protocol for on-field quantity of explosives using the SPR sensor. The effectiveness of the SPR immunosensor for explosive detection, but it does not provide a methodical explanation of the intricate process of interaction between the antibody-based recognition unit and TATP molecules. Instead of elucidating the fundamental signal transduction process responsible for SPR response production, the study concentrates more on sensitivity and detection efficiency. Little research has been done on the nanomaterials might improve surface contact, signal amplification, and plasmonic activity. There is still a lack of discussion on the internal mechanisms of charge transfer, refractive index change, and molecule adsorption at the sensor surface. The testing procedure is mostly dependent on controlled laboratory settings and is not evaluated in the presence of actual environmental interferences such humidity, mixed vapors, and field-level pollution. Additionally, practical constraints such as sensor stability, repeatability, portability, and long-term operating performance were not fully addressed.

The detection of non-conventional explosive components such as TATP and HMTD has become a significant concern due to the rise in global terrorist activity. Dogs were successfully utilized to sense narcotics and conservative, extreme explosives. Oxley and colleagues[49] found that dogs could also detect hard TATP and TATP adsorbed on cotton balls. They developed an operative method for training dogs to sense TATP by using cotton balls infused with TATP vapor. Under various conditions, it had been found that dogs could detect as little as 200.0 μg of TATP adsorbed onto a 1 g cotton ball. However, TATP tends to rapidly vaporize at room temperature, leading to momentous depletion from the cotton balls in as little as 20 min, thereby hindering the dogs' aptitude to sense it. To address this issue, TATP-depleted cotton balls could be recharged by placing them in a closed ampule containing TATP residue for ~ 20 min. Under controlled circumstances, the behavioral performance of trained dogs for TATP detection was presented, along with detection success rates. The chemical interaction mechanism between TATP vapors and the canine olfactive recognition system was crucial. There is a lack of detailed discussion of the fundamental concepts of signal recognition and odor-response pathways. The report does not analyze sensing techniques based on nanomaterials that might improve artificial detection systems' sensitivity, selectivity, and signal amplification. Reproducibility and dependability may be impacted by the testing method's practical limits, which also include reliance on canine training quality, weariness, ambient factors, and handler influence. Compared to more sophisticated portable sensor technologies, the approach is less appropriate for large-scale real-time field analysis and continuous quantitative monitoring.

3.1.2. Mass Spectrometry

With Headspace Gas Chromatography Mass Spectrometry

Stambouli et al.[50] demonstrated a novel analytical technique for sensing TATP residues in post-explosion debris samples using an *Headspace Gas Chromatography Mass Spectrometry* method. The chromatogram, obtained after inserting 1000.0 µL of HC- explosion- wreckage showed the TATP-peak at 13.18 min, with a mass-spectrum considered by an ion mass/charge [M^{-1}] 221 or 3- other fragments 43 $[C_2H_3O]^+$, 59 $[C_3H_7O]^+$, & 75 $[C_3H_7O_2]^+$, confirming the explosive's molecular structure. Additionally, at 5.80 min, indicated Diacetone Diperoxide was observed adjacent to the TATP peak. Throughout the analysis, a track of the TATP peak was observed, caused by heat degradation at the injector level. To prevent degradation of the analyte, the temperature of the injection-port was decreased from 270 °C- 110 °C. The LOD was 0.1 ng. The detection effectiveness of TATP traces in post-explosion debris using this analysis is demonstrated. It does not fully elucidate the interaction mechanism between TATP molecules and the detection system. Without addressing the fundamental signal conversion concepts involved in chromatographic and mass spectrometric detection, the study mainly presents analytical sensitivity and identification results. Insufficient analysis has been done on the internal processes pertaining to ionization behavior, fragmentation paths, and molecular interactions during detection. Practical drawbacks of the testing approach include costly equipment, difficult sample preparation, the need for a professional operator, and restricted mobility for on-site real-time analysis. Reproducibility may also be impacted by matrix complexity, environmental interference, and low trace concentration in post-blast residues.

A method for identifying TATP residues in liquid samples (aqueous TATP synthetic waste) and in the gas phase is presented by Hehet et al.[51] Gas chromatography-mass spectrometry (GC-MS) or GC with positive chemical ionization and tandem MS (GC-PCI-MS/MS) analytical techniques are used to identify the explosive after TATP is enriched from the aqueous or gas phase using various passive samplers (polydimethylsiloxane (PDMS) sampling rods and activated carbon sampling tubes (ACST)). This work has also investigated the stability of TATP in aqueous solutions, the stability of enriched TATP in passive samplers under various storage settings, and the development of TATP re-extraction techniques from passive samplers.

Proton transfer reaction mass spectrometry

Proton transfer reaction mass spectrometry (PTR-MS) detects in different compounds by changing the discharge gas, producing various reagent ions in the ion source. Zhang et al.[27] developed a new method, called ammonia-assisted PTR-MS, to modify reagent ions. Ammonia was introduced into a temporary PTR-MS device through an injection port bypass. The traditional PTR-MS apparatus using

H_3O^+ $(H_2O)_n$ (n = 0, 1, 2) reagent ions could be converted to an ammonia-assisted PTR-MS with NH_4^+ reagent ions. When the conventional PTR-MS closed the injection port, bypassing ammonia flow, 7.58 ppm TATP steam was injected into it. The ion $[TATP+H]^+$ with a mass-to-charge ratio of 223 was selected as the distinctive ion. The drift tube voltage was adjusted in increments of 10 V, ranging from 50 V to 240 V. As the voltage of the drift tube increased, the strength of the ionic signal of $[TATP+H]^+$ fluctuated and peaked at 140 V. When using traditional PTR-MS for TATP detection, the sensitivity increased by more than 37 times, and the limit of detection was as low as 1.3 ppb. The exact interaction mechanism between TATP molecules and the ionization/reaction species is not comprehensively explained by ammonia-assisted proton transfer reaction mass spectrometry (PTR-MS), despite its analytical efficacy for TATP detection. Rather than elucidating the basic signal conversion mechanism involved in proton transfer and ion production, the study mainly concentrates on detection sensitivity and spectrum response. There is no discussion of how nanomaterials might improve signal amplification, ionization efficiency, or adsorption. Internal processes pertaining to charge-transfer routes, molecule fragmentation, and ammonia-assisted ion chemistry are still not fully understood. Practical limits of the testing approach include the need for highly skilled individuals for analysis, regulated working conditions, and sophisticated apparatus. Its broad practical use for on-site TATP detection may however be limited by problems including high operating costs, restricted mobility, environmental interference, and difficulties with real-time field deployment.

$$NH_3 + H_3O^+(H_2O)_n \rightarrow NH_4^+ + (H_2O)_{n+1} \quad \text{.....(1)}$$

$$TATP + NH_4^+ \rightarrow [TATP + NH_4]^+ \quad \text{.....(2)}$$

Desorption electrospray ionization (DESI) mass spectrometry

DESI is a sensitive and selective ionization technology that detects tiny levels of peroxide-based explosive TATP on ambient surfaces. Complex formation with alkali ions (Li^+, Na^+, and K^+) facilitates this process. Collision-induced dissociation (CID) of TATP-metal complexes results in the retention of metal in fragment ions. To explain the fragmentation of TATP's alkali metal complexes and interpret the CID spectra, a mechanism that aligns with observed data and independent labeling studies. The initial stage in the CID fragmentation process is homolytic breakdown of the fragile peroxide bond O-O (34-37 kcal/mol) to form a biradical. Later, rearrangement occurs by two methyl shifts from neighboring carbons to the oxygen radical sites.[Fig. 2] After homolysis of the O-CH3 bond, the methyl groups are freed, leading to recombination and the production of ethane. The ion at m/z 245 fragments to generate a product ion at m/z 215 ($C_7H_{12}O_6$ + Na).[52]

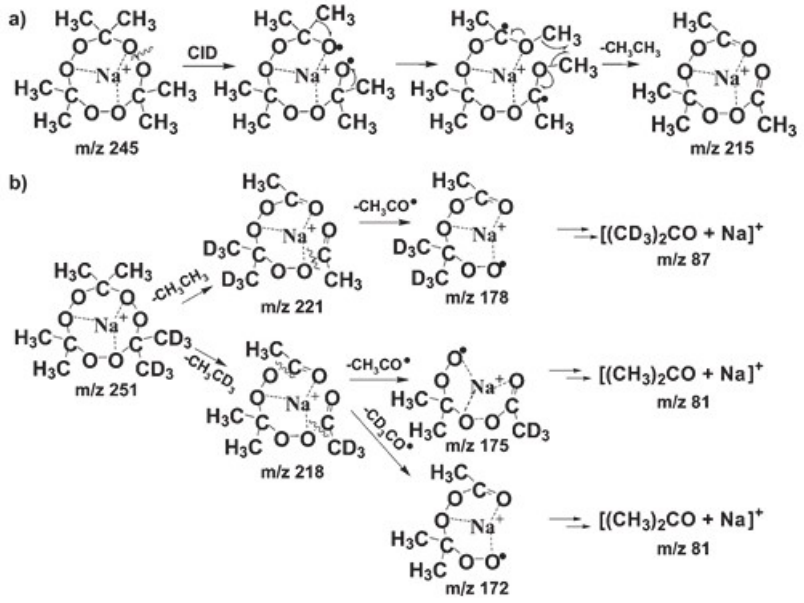

Fig.2: Proposed mechanism for dissociation of (a) the (TATP +Na)⁺ complex at m/z 245 and (b) the deuterated complex (TATP + Na)⁺ at m/z 251.(reprinted with permission Cotte-Rodrı´guez et al.[52]).

3.1.3 Cavity ring-down spectroscopy

Taha et al.[53] used thermal decomposition peroxy radical chemical amplification cavity ring-down spectroscopy (TD-PERCA-CRDS) to detect TATP by thermal breakdown of peroxy radicals. This approach involves sampling air through a heated intake and adding approximately 1 ppmv of nitric oxide (NO). To ensure the quality of synthetic standards, the mid-infrared spectrum of TATP vapor was measured. TATP's thermal breakdown generates radicals that oxidize NO to NO_2. The concentration of NO_2 is measured at 405 nm with a blue diode laser CRDS. Adding approximately 1% ethane (C_2H_6) improves sensitivity and catalyzes the conversion of NO to NO_2. The detection limit of TD-PERCA-CRDS for TATP is 22 pptv , which is almost six orders of magnitude lower than TATP's saturated vapor pressure. This article discusses the mechanics of TATP thermal decomposition, TD-PERCA-CRDS interferences, and its usefulness for detecting peroxy radical explosives at security checkpoints. TATP's major breakdown route is non-redox and includes many acetone elimination stages to produce O_3. The first equivalent of acetone produces an alkoxy peroxyl diradical intermediate species (I). The diradical forms a 7-membered ring (II) before being thermally decomposed into acetone and an alkoxy trioxyl diradical (III). This molecule produces a third equivalent of acetone and an O_3 molecule. When the alkoxy peroxyl diradical (I) reacts with NO, it likely forms the dialkoxy diradical (IV). This molecule is a ring opening product of DADP and may undergo a C-O cleavage process to delete two acetone molecules and one O_2 molecule. This process produces one equivalent of NO_2 per TATP and is identical to the mechanism. These routes do not explain the observed amplification in the presence of NO and ethane, which need radicals to feed into the PERCA reaction chain. To explain the production of such radicals, They hypothesize that (IV) undergoes a C-C cleavage process to yield a methyl radical

and an intermediate (V). This molecule can undergo a C-C cleavage process, resulting in two more methyl radicals. In NO^-only mode, the methyl radical undergoes reactions R_1, R_3, R_5, and R_2 to create two equivalents of NO_2. This route results in seven equivalents of NO_2. Alternatively, (V) can remove acetone to produce the PA radical, which transforms NO molecules to NO_2.

3.1.4. Ion mobility spectrometry (IMS)

Fan and colleagues[54] conducted a study where they showed that using a new planar solid-phase microextraction (PSPME) as a preconcentration and sampling device for headspace analysis was more sensitive and efficient than the conventional fiber-based solid-phase microextraction (SPME) followed by ion mobility spectrometer (IMS) detection, specifically for TATP. TATP standards were utilized to quantify and compare the retention capacities of PSPME to commercially available SPME. Gas chromatography-mass spectrometry was used for SPME analysis, whereas a commercial IMS with no instrumental modification was used for PSPME. To determine the shortest extraction time for identifying a 10 mg TATP sample, static extraction times were tested at room temperature. TATP was detected in the headspace of a half-gallon glass container after a 1-minute extraction at room temperature. TATP was detected using a combination of static and dynamic extractions. The detection was done by sampling and pre-concentrating TATP on a PSPME device in less than 30 seconds. A readily available commercially feasible IMS was used to identify TATP without requiring any changes to the sample intake. IMS produced fast sample and detection times for TATP detection, which made it appropriate for field analysis with high sensitivity and selectivity. Fiber-based SPME sampling took 22 min, whereas TATP sampling and analysis only required around 35 seconds. PSPME increases TATP recovery from 5% to about 20% compared to fiber-based SPME. The ability to quickly detect TATP utilizing planar solid-phase microextraction (PSPME) in conjunction with ion mobility spectrometry (IMS), but it does not provide a comprehensive explanation of the intricate process of interaction between TATP molecules and the extraction or sensing surface. The paper very briefly discusses the fundamental signal conversion mechanism used in IMS analysis, focusing instead on sensitivity, extraction efficiency, and detection speed. Furthermore, the impact of nanomaterials in enhancing signal amplification, selectivity, and adsorption capacity is not well investigated. It is still unclear how vapor adsorption, ionization behavior, and ion mobility response work internally. Practical drawbacks of the testing procedure include its vulnerability to environmental influence, the effects of humidity, and the potential for false-positive results from chemicals that are chemically identical. Additionally, its mobility and large-scale real-time field use may be limited by the need for specialized instruments, calibration techniques, and regulated working conditions. A PSPME device had a cross-section width of ~324 μm, whereas an uncoated glass filter had a cross-section width of approximately 347 μm. The fact that there was no increment in cross-sectional width showed that the sol-gel-based PDMS was well integrated into the glass-filter surface. Likewise, surface scans show that the width of

the glass-fibres in PSPME has grown by ~2 µm, increasing competence and phase volume. Surface-analysis investigations demonstrated that the surface area of the glass filter after covering decreased from 5.245 m^2 /g (uncovered glass filter) to 2.197 m^2 /g (covered glass filter), which was consistent with the width capacities of the PSPME in the Keyence digital microscope.[28]

These substances include hexamethylene triperoxide diamine (HMTD) and triacetone triperoxide (TATP). Despite the significant variation in vapor pressure extremely high for TATP and very low for HMTD an effort was made to build a device that would enable the simultaneous detection of both chemicals. The proposed technology combines a particularly built gas sample injection device with differential ion mobility spectrometry (DMS). The developed detector technology made it possible to identify a very low quantity of HMTD and a large concentration of TATP. Despite the presence of impurities acetone that was left over from the technical process and developed as a coproduct of the manufacture of diacetone diperoxide (DADP)—TATP detection was still feasible. The exact interaction mechanism between explosive chemicals and the ionization or recognition system is not systematically explained by the detection performance of TATP and HMTD utilizing Differential Ion Mobility Spectrometry (DMS). The article very briefly discusses the fundamental signal conversion mechanism involved in ion mobility separation, focusing instead on detection sensitivity and mobility responsiveness. Furthermore, the potential of nanomaterials to enhance signal amplification, ion transport, selectivity, and adsorption efficiency is not well investigated. There is still much to learn about the internal processes behind ion production, charge transfer, clustering behavior, and mobility differentiation. Sensitivity to humidity, environmental interference, and overlapping signals from chemically related chemicals are some of the testing method's practical drawbacks. Large-scale real-time field applications and mobility may be restricted by the need for complex instrumentation, calibration processes, and regulated operating conditions [23].

With minimal instrumental effort, High Kinetic Energy Ion Mobility Spectrometry (HiKE-IMS) is a flexible method for detecting gaseous target molecules that is very helpful in complicated chemical environments. By operating HiKE-IMS at lower pressures (between 10 and 60 mbar) than at ambient pressure, less ion-neutral collisions occur, which lowers chemical cross-sensitivities and does away with the requirement for an earlier separation step, such as gas chromatography. Furthermore, HiKE-IMS can operate over a broad range of reduced electric field strengths E/N up to 120 Td. This enables the separation of ions by low-field ion mobility and takes advantage of the field dependence of ion mobility, which may enable the separation of ion species at high E/N despite comparable low-field ion mobilities. These benefits make HiKE-IMS a potential tool for trace gas analysis, including the detection of triacetone triperoxide (TATP). HiKE-IMS was used in this investigation to identify TATP. The field-dependent ion mobilities and the ionization of TATP, offering a database of the ion mobilities based on E/N. Ionization of TATP by proton transfer with H_3O^+ in HiKE-IMS produces fragments,

confirming the results reported in the literature; however, utilizing NH_4^+ as the major reactant ion results in the TATP·NH_4^+ adduct. This adduct fragments at high E/N, which may offer more details for accurate TATP detection. The exact interaction mechanism between TATP molecules and the ionization or sensing system is not systematically explained by the detection performance of TATP employing High Kinetic Energy Ion Mobility Spectrometry (IMS). Sensitivity, ion mobility behavior, and analytical efficiency are the main findings of the study; the fundamental signal conversion concepts involved in IMS detection are only briefly discussed. Furthermore, the potential of nanomaterials to enhance signal amplification, ion transport, selectivity, and adsorption efficiency is not well investigated. There is still much to learn about the internal processes behind ion production, fragmentation behavior, charge transfer, and mobility separation. Sensitivity to humidity, ambient interference, and overlapping ion signals from chemically related chemicals are some of the testing method's practical drawbacks.[55]

3.1.5. Thermodynamic based gas sensor

A small-footprint gas sensor was fabricated by Amani et al.[28] that can detect the heat of the reaction during the catalytic decomposition of TATP, by utilizing metal oxide catalysts, could detect the heat of the reaction during the catalytic decomposition of TATP. The percentage of reactivity to 8 ppm TATP and 9 ppm H_2O_2 was determined through static testing at various temperatures. A significant drop in the response for tin oxide occurs below 300°C, followed by a sharp increase in response as the temperature rises. A peak reaction occurs at around 400°C because of the catalyst breaking down TATP. The reaction to hydrogen peroxide was quite like the TATP reaction when using the same catalyst. Below 380°C, there was no noticeable reaction. However, the rate of reaction increased significantly, peaking at 460°C. The response to 8 ppm TATP was measured using static testing. The response was analyzed as a function of temperature with the use of various catalysts such as WO_3-TiO_2, V_2O_5, SnO_2-x, Nb_2O_3, and ZnO. The results showed that the temperature-dependent responses of the oxide catalysts varied. Among the five catalysts, Nb_2O_3 exhibited the least peak response, while ZnO displayed distinct peaks. The target gas was expected to contain a combination of air and TATP vapor, along with some H_2O_2 vapor due to the catalytic breakdown of TATP. The thermodynamic-based gas sensor's detection efficiency for TATP vapor analysis, but it does not provide a methodical explanation of the intricate process of interaction between TATP molecules and the detecting surface. The research gives little attention to the fundamental signal conversion concepts that underlie detection, instead concentrating mostly on sensor response and thermodynamic behavior. Furthermore, a thorough analysis of how nanomaterials improve adsorption capacity, thermal responsiveness, sensitivity, and selectivity is lacking. It is still unclear how heat transmission, molecule adsorption, and physicochemical interactions work internally at the sensor interface. Additionally, the testing method has practical limits, such as susceptibility to ambient conditions that may impact detection accuracy, such as temperature, humidity,

and interfering vapors. Furthermore, problems with repeatability, real-time field deployment, calibration needs, and long-term sensor stability were not fully addressed.

3.1.6. Electrochemical detection of TATP

Capua et al.[29] showed the device enclosed sensitivity to TATP vapors at varied concentrations. TATP was evaporated in a sealed room before being diluted with nitrogen. Because it was impossible to acquire concentrations below 100 ppb with sufficient precision, the lowest [TATP] found was 100 ppb. The detection limit appears to be caused mostly by electrical noise. They demonstrated that the presence of H_2O_2 in the gas does not affect its sensitivity to TATP, even when the concentration of H_2O_2 was a hundred times higher than that of TATP. TATP effectively interacts with the surface states in GaAs, changing the surface potential and current flowing through the device. When GaAs is oxidized, the oxide layer either removes or prevents the surface state from interacting with TATP. As a result, the oxidized GaAs device is not responsive to TATP. Although the work emphasizes the analytical potential of sensor arrays for TATP vapor identification through pattern-based responses, it does not provide a detailed description of the molecular-level binding mechanism between the analyte and sensing surface. Sensitivity and classification accuracy are prioritized over elucidating how chemical adsorption generates quantifiable electrical outputs. The sensing platform incorporates sophisticated materials, although their role in electron transport, surface activation, and response amplification is barely acknowledged in passing. Important phenomena including energy-transfer mechanisms, diffusion channels, and intermolecular interactions are still not fully understood. During real operation, interference from moisture, temperature fluctuations, and volatile organic substances may also affect the experimental technique. Furthermore, issues with mobility, constant on-site monitoring, calibration consistency, and device durability were not thoroughly examined.

A molecularly imprinted polymer (MIP) with electrochemical capabilities was developed for the sensitive and selective determination of TATP. Molecular imprinting had been achieved through electro-polymerization on the surface of a glassy carbon electrode. A pyrrole functional monomer, TATP template, and $LiClO_4$ were used to create a polymer film from a solution. Cyclic voltammetry was employed to create the film. Differential Pulse Voltammetry was performed on TATP using $LiClO_4$ as a supporting electrolyte. The test was conducted in a potential range of -2.0 V to +1.0 V (versus Ag/AgCl). Three-factor two-level factorial design was used to optimize the monomer concentration at 0.1 $mol \cdot L^{-1}$, template concentration at 100 $mmol \cdot L^{-1}$, and the number of cyclic voltammetry scan cycles to 10. The TATP-MIP sensor and bare glassy carbon electrode had different analytical characteristics. The TATP-MIP sensor had ppb detection and quantification limits, which make it suitable for trace analysis. The glassy carbon electrode had a limit of detection of 26.9 $\mu g \cdot L^{-1}$ and a limit of quantification

of 81.6 μg·L^{-1}. These values were well within the ppm range, which makes the GC electrode less suitable for trace-level analysis. The GC electrode's range was 12,300-222,500 μg·L^{-1} with a correlation coefficient $R^2 = 0.966$, well within mid ppm levels.[35]

Based on its acid treatment

Munoz et al.[36] reported a rapid, easy, and sensitive electrochemical approach for sensing peroxide-based explosives using acid treatment. They showed that adding acid-treated acetonitrile and TATP solutions resulted in current-time records at the Prussian blue-adapted glassy-carbon electrode (controlled at 0.00 V). The sensor responds quickly to the addition of 2 μM. In combination with a 15-second acid treatment and a 5-second neutralization, well-defined peroxide-reduction currents with minimal noise and speedy responsiveness were obtained. TATP was converted to hydrogen peroxide at faster rates when the acid content was higher. Between 0 and 3 M HCl, the current increases quickly; after that, it increases more slowly. The signal rises as the volume ratio increases between 0.30 and 1 and practically stops at larger ratios. For an effective conversion, it appears that a great acid/TATP molar ratio was necessary (with a concentration of the TATP sample playing a small role, likened to the necessity for a greater quantity of hydrochloric acid). Factors influencing the efficiency of TATP acid pretreatment were investigated and optimized to allow sensitivity measurement as low to the 50 ng level in 60 seconds. The quick electrochemical measurement of TATP following acid-induced breakdown, however it offers little insight into the molecular mechanisms behind analyte identification and response production. The molecular pathway between peroxide breakdown and electrochemical signal production receives less attention than analytical output and sensor efficiency. It is not well understood the catalytic surfaces, electron-transfer kinetics, and interfacial processes contribute to current fluctuation. Furthermore, there is still a lack of research on nanostructured materials affect signal amplification, active-site availability, and conductivity augmentation. Under realistic operating circumstances, the experimental technique may also be hampered by matrix contamination, acidic interference, and instability of breakdown products. Furthermore, further real-time and field-based deployment may be limited by reliance on controlled laboratory, calibration sensitivity, and potential repeatability problems. It followed two types of measurement

(A) Amperometric observations: neutralisation of the acid that converts TATP

In combination with a rapid acid conversion of peroxide explosives to H_2O_2, an extremely lively, sensitive, selective, and steady Prussian blue electrocatalytic transducer might be observed.

(B) Chronoamperometric observations without neutralisation: acid conversion of TATP

Direct electrochemical capacities of the H_2O_2 product without further neutralization in the very acidic media used to produce it.

3.1.7. Fluorogenic detection of TATP

The conversion of boronate esters to the equivalent phenols/phenoxides by hydrogen peroxide has often been explored in solution or in biological systems for hydrogen peroxide detection. There have been fewer reports of fluorescence-based detection of hydrogen peroxide, and hence TATP, in the solid form.

Quenching-based detection

Almenar and colleagues[56] synthesized 2-dansyl-adapted cyclodextrin-derivatives (1 and 2) [Fig. 3] to build host-guest sensory schemes for the shortest fluorescence sensing of the H_2O_2, DADP, and TATP in aquatic circumstances. When ^{1}H-NMR spectra were taken in the presence of TATP, there were relatively few changes in the cyclodextrin signals. There were no gestures relating to Diacetone Diperoxide or TATP in the ^{1}H-NMR spectra in D_2O in the absence of cyclodextrin, which was consistent with the relatively poor solubility of these peroxide explosives in aquatic systems. At ambient temperature, both composites showed a significant decrement in luminescence intensity in the presence of peroxide. Diacetone Diperoxide had a larger impact than TATP in both sensors. To recover the sensitivity, they heated the sensor R-O-O-R mixture at 40 ^{o}C for 10 min and discovered that the sensitivity to TATP could be notably enhanced, and sensor 1 exhibited a decrement in luminescence intensity of approximately eleven percent in the existence of surplus TATP and approximately 7 % in the presence of Diacetone Diperoxide. The chemical recognition mechanism between TATP and the supramolecular receptor is not fully described, despite the fluorogenic sensing capability for peroxide explosives through host–guest interactions. Fluorescence response and detection efficiency are more important than explaining how guest binding causes optical signal production. Only a few key points are covered, including energy transmission, electronic disturbance, and binding-induced photophysical changes. The significance of nanostructured platforms to response stability, adsorption behavior, and fluorescence amplification is not extensively examined, despite the demonstration of selective recognition. Under real-world circumstances, the analytical process may also be hampered by competing volatile chemicals, ambient dampness, and poor host-guest affinity. Furthermore, issues with operational repeatability, mobility, long-term sensor durability, and suitability for ongoing field monitoring were not fully assessed.

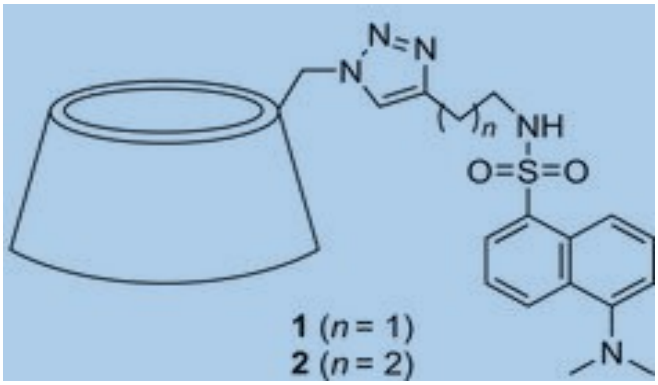

Fig. 3: Compounds 1 and 2 are structured and synthesized. (reprinted with permission Almenar et al.[56]).

Enhancement-based detection

The visible fluorescent method for TATP detection was described by Malashikhin et al.[30] TATP did not have a direct reaction with pro fluorophores. It reacted quickly with hydrogen peroxide, produced by UV irradiation of TATP, causing oxidation to the respective sulfones in the presence of methyltrioxorhenium (MTO). The chemical processes controlling analyte recognition and optical response production are not fully explained by the fluorescence signaling performance of sulfoxide profluorophores for TATP identification. The focus of the discussion is on visual detection sensitivity and capacity, with little emphasis paid to the photochemical processes that cause fluorescence activation. Significant elements including excited-state behavior, oxidation routes, and electron redistribution during signal creation are still not well understood. The role of nanoscale materials to emission amplification, surface confinement, and stability improvement is not well investigated, despite the demonstration of selective sensing. Under actual operating circumstances, the analytical technique may additionally face challenges from interfering oxidizing species, ambient humidity, and the instability of fluorescent intermediates. Additionally, problems with quantitative dependability, long-term preservation, repeatability, and flexibility for portable field deployment were not well addressed.

One potential disadvantage of this tactic was that 2b–4b [Fig. 4] were stable under visible light, but not under prolonged UV irradiation. Radical fragmentation and recombination were necessary for the signalling process. However, 2b oxidized to 2c while maintaining a significant fluorescence increase, indicating that structural modification might be possible to reduce deterioration without surrendering significant fluorescence response. It also degraded more slowly than 3b or 4b. Starting with 500 nanomoles (about 0.10 mg) of TATP photolysis, a five-fold increment in visual luminescence was achieved in 50 min. In terms of detection limitations, they discovered that they could induce a visible

reaction to as low as 100-nmole of TATP. Even though an extended response time (90 min) was required for completion, the luminescence could still be shown with the naked eye.[57,58] In the example of $C_{14}S_{14}OS$ (benzylic sulfoxides) 3b and 4b,[30] precedence indicated an R-cleavage recombination pathway as the primary non-radiative deactivation mechanism for the excited-state, rather than photo-induced electron transfer (PET) quenching. Sulfones had a stronger C-S bond than sulfoxides. It might be concluded from a comparison of $(CH_3)_2SO$ and RS(=O) 2R' that this deactivation process was inhibited in the corresponding sulfones. Although there were differences in the emission from sulfides 2a to 4a, even in the less emissive situations of 3a & 4a, sulfides were more emissive than the comparable sulfoxides. In 3a and 4a, the R-cleavage also took place, but less effectively than in the sulfoxides.

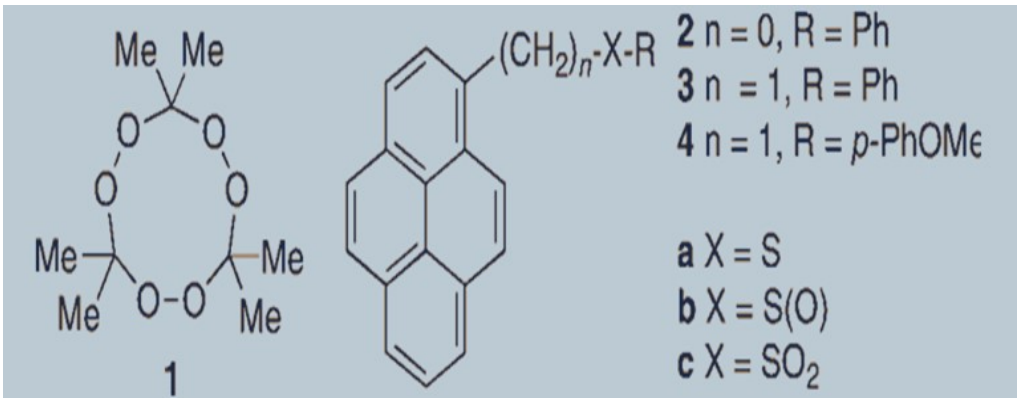

Fig.4: TATP with Pro-fluorescent probes. (reprinted with permission Malashikhin et al.[30]).

Fan et al.[31] demonstrated the synthesis and sensing of 2,4-diuorophenyl or 4-trifluoromethylphenyl units, which were intended to improve the conjugation duration of the chromophore compared to the parental fluorenylboronate ester. They evaluated the photo-physical aspects of the materials. They could sense TATP in the solid state quickly. There was an increase in absorption at longer wavelengths in both instances. A significant rise in the photoluminescence signal attributed to the produced phenoxide was noticed upon photoexcitation at a wavelength that the boronate ester did not absorb, confirming the detection of hydrogen peroxide. They compared the UV and photoluminescence spectra of phenoxide(1-O), which was produced directly from 1-OH, with those of the product generated via the reaction between 1 and TATP. The similar spectra demonstrated that boronate esters were transformed into the corresponding phenoxides. Within seconds, each component exhibited a definite reaction to the TATP vapor. The rate of photoluminescence was proportional to the concentration of TATP vapor. The limit of detection for films of compounds 1 and 2 was determined to be approximately 40 and ~2.5 ppb

for TATP, respectively, based on the photoluminescence intensity alteration in the first 60 seconds. Although the quick fluorescence-based indirect sensing efficiency for TATP detection is effective, the molecular-level mechanisms behind analyte identification and optical response production remain unclear. Rather than describing how peroxide breakdown causes fluorescence modulation, the topic is mostly focused on analytical sensitivity and response speed. Important elements that affect emission behavior, including as chemical intermediates, photophysical transitions, and electronic interactions, are still not well understood. The impact of nanostructured materials on adsorption kinetics, energy transfer, and signal reinforcement is very briefly discussed, despite reports of improved sensing performance. Interfering oxidants, ambient moisture, and reactive species instability during practical operation can all have an impact on the experimental process. Furthermore, issues with calibration dependability, storage stability, device repeatability, and appropriateness for ongoing field-based monitoring were not thoroughly evaluated.The addition of electron-withdrawing groups improved the materials' resistance to photodegradation, which in turn raises the sensitivity of the sensing process since the turn-off impact of photodegradation was less severely concealed by the turn-on signal. Fan et al.[31] analyzed the relative sensing kinetics of the 2-materials (2,4-difluorophenyl or 4-trifluoromethylphenyl), since photo-degradation processes were significantly slower than TATP "turn-on" detection. They compared the sensing kinetics rate of change of films 1 and 2. Complex 2 demonstrated the fastest rate of photoluminescence changes across all TATP concentrations, which might be attributed to its better photostability of phenoxy species (2-O^-).

Fan et al. [32] studied thin films based on fluorenyl boronate ester chromophores for the detection of TATP vapours via the decomposition product, H_2O_2. The absorption spectra for the sensing film mix earlier and afterward 150 seconds of exposure to TATP (derived from 8 ppm TATP). The absorption increased at longer wavelengths. For composites one and two, the rate of photoluminescence was proportional to [TATP-vapor]. The LOD for films of compound two was 40 ppb for TATP based on the photoluminescence intensity alteration in the first 60 seconds. The rate of rise in photoluminescence with increasing TATP concentration was not the same for dendrimer 3 [Fig 5], which they attribute to film aggregation, dendrimer lipophilicity, and a delayed reaction rate. TATP was introduced to films of 2 or 3 for 180 to 250 seconds, and the photoluminescence was measured through the first phase. Before reilluminating the film, the excitation was turned off for 10 min after the analyte pulse. The photoluminescence signal in the film containing compound 2 changed slightly, but the photoluminescence in dendrimer 3 grew dramatically, showing that the oxidation reaction continued in the dusky afterward the pulsation ended. The photoluminescence did not decline to a similar point throughout the period. Photo-degradation was shown to be at least partially responsible for the decline in PL with time (at 5.30 ppm [TATP vapor]). Compounds 2 and 3 both showed slower photo-degradation than compound 1, owing to the existence of the −C ≡ N group. There was a rivalry in the sensing process between "turn on" sensing and the following breakdown of the emissive phenoxide.

Photo-degradation had no effect on the materials' capacity to detect TATP. According to Fan et al.,[33] adding a -RCN group to the fluorenyl ring dramatically increments the phenoxides and absorption while also enhancing their photostability. The generation of phenoxide and photo-degradation, the latter of which was a slower process and does not alter the capacity to sense peroxide, were shown to be the two mechanisms controlling the kinetics.

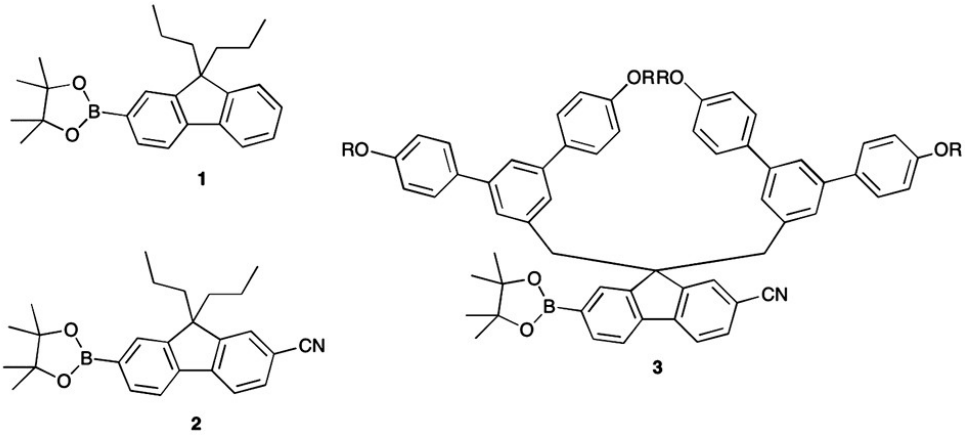

Fig.5: Structure of the sensing materials. (reprinted with permission Fan et al.[31]).

For hydrogen peroxide and organic peroxides like TATP, Germain et al.[33] created a very sensitive turn-on luminescence detection technique. The LOD for hydrogen peroxide and TATP was 10 nM. When H_2O_2 was added directly to the pro chelator/Zn^{2+} solution, the fluorescence signal increased 800-fold (left axis). For 5 minutes, diluted TATP (10 M to 10 nM) was combined with acetic acid (0.5 M) in MeOH. The fluorescence signal (λ_{em} 440 nm) increased approximately 80-fold [Fig. 6] when each TATP/H^+ solution was added to a typical pro chelator/Zn^{2+} solution. With a detection limit of less than 10 nM. The turn/on luminescence detection technique identified simple peroxides as well as TATP. Schiff-base hydrolysis followed by salicylaldehyde oxidation to salicylic acid was one possible degradation pathway; however, the fluorescence peak and decrease indicate that the degradation mechanism was more intricate. The chemical recognition mechanism responsible for fluorescence activation is not fully explained by the "turn-on" fluorescence response for detecting H_2O_2 and TATP. While offering little insight into the underlying photochemical and electronic transition mechanisms, the discussion mostly concentrates on sensor sensitivity and emission enhancement. Only a few key processes are discussed, including excited-state modulation, peroxide-induced oxidation, and fluorescence recovery routes. The impact of nanoscale designs to surface contact, charge migration, and optical amplification is still not fully understood, despite the demonstration of better analytical performance. Under real-world circumstances, competing oxidizing agents, air humidity, and the instability of reactive intermediates might all offer problems for the suggested technique. Additionally,

factors pertaining to portability, quantitative repeatability, long-term operational consistency, and suitability for ongoing on-site monitoring were not fully investigated.

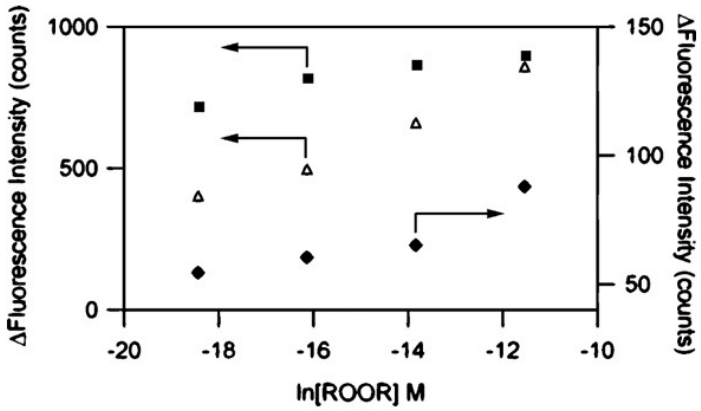

Fig.6: The relative fluorescence rise of prochelator/$Zn(OAc)_2$ (3 mM in MeOH) to peroxide.(reprinted with permission Germain et al. [33]).

An et al.[59] designed a fluorescent compound-based test paper with excellent sensitivity, rapid reaction times, and complete reversibility for detecting TATP and its acetone breakdown product in the gas phase. The azetidine group was used to generate the naphthalene diimides (NDI) [60,61] derivative known as DNNDI, which not only increased the fluorescence quantum yields of NDI but also increased their photochemical stability.[63-65] The acetone and TATP vapours responded impressively to DNNDI-based sensing sheets, and noncontact visualization detection of TATP was also possible. At room temperature, TATP easily broke down and released acetone due to its poor chemical stability. TATP vapor was detected at various concentrations (0.50 mg/ mL, 1 mg/ mL, 2 mg/ mL, 4 mg/ mL, and 8 mg/ mL), and every single test was performed three times. The luminescence signal of the film-based detector at varying concentrations of TATP vapor indicated a progressive increase in response strength with an increment in the attentiveness of TATP vapor.[62] The amount of reaction was positively correlated with the amount of TATP vapor (R^2=0.997). An et al.[59] demonstrated that solvent vapor significantly disturbed the connection between solid molecules, weakening the aggregation-stimulated quenching effect**.**

Eu-MOF with nonfluorescent emission was created by modifying the amount of hydroxyl groups in ligands to improve signal-to-noise ratio, sensitivity, and reaction speed with triacetone triperoxide (TATP). The reaction was triggered by H_2O. Selecting 2,5-dihydroxyterephthalic acid (DHTA) as the ligand and adding H_2O resulted in a weaker intermolecular hydrogen bond that was interrupted and oxidized from the original enol structure to a ketone, resulting in a fluorescence turn-on response to TATP. The Eu-MOF exhibited high-performance sensing for TATP, with fast response (< 1 s), low

limit of detection (LOD, 36.1 nM), superior selectivity even in the presence of 28 types of interferents, including hydrogen peroxide, strong robustness, and the ability to detect 5 pg airborne TATP particles. They tested the practical practicality of the Eu-MOF by integrating a sensor chip into a portable detector. This confirms its promise for trace-level TATP detection in real-world applications. Using the intersystem crossing (ISC) mechanism, an approach for generating nonfluorescent MOFs has been developed to increase signal-to-noise ratio, sensitivity, and reaction time towards analyte by adjusting the quantity of hydroxyl groups in organic ligands. To better understand the sensing mechanism of Eu-MOF-3 to TATP, the ligand DHTA was transformed to DM-DHTA using an esterification procedure. This allowed for simulation of the ligand structure in Eu-MOF-3 [Fig. 7]. The natural bond-orbital technique was used to investigate the parameters that influence the enol structure's reactivity to TATP before and after H_2O addition.[66]

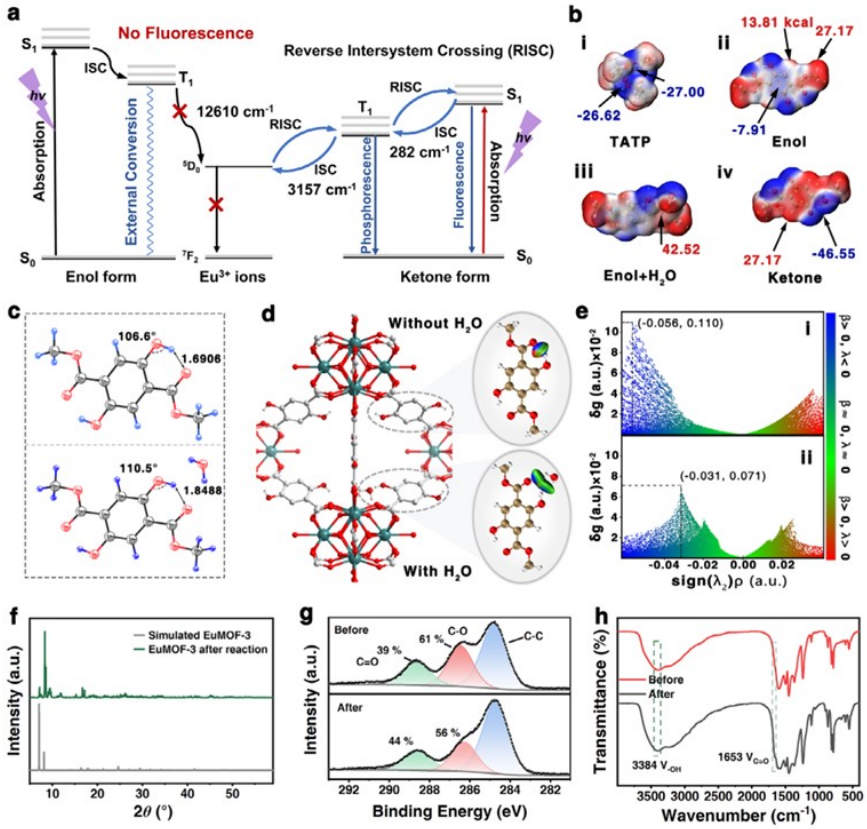

Fig.7: Sensing mechanism of the Eu-MOF-3 toward TATP. (reprinted with permission Cheng et al.[66]).

3.1.8 Colorimetric detection of TATP

Colorimetry is another easy approach for detecting peroxide explosives on-site in a quick, qualitative, and selective manner. Colorimetry detection of TATP has mostly focused on colorimetric

sensors and colorimetric sensor arrays. These approaches offer great sensitivity, selectivity, and analytical speed, as well as provide trustworthy qualitative results. Colorimetry yields very few results for detecting TATP.

A sensing platform, reported by Lin et al.[67], could identify even very small amounts of TATP fume colorimetrically from its corrosive breakdown products (for example, hydrogen peroxide), even as low as 2 ppb using an acid catalyst and dyes. They used a normal flatbed scanner to take digital pictures of an array earlier and afterward, applying different quantities of TATP vapor. It was possible to map color (red, green, and blue) of each point with TATP vapour concentration. Such a color-based sensing array was able to semi-quantitatively detect TATP vapor at concentrations as low as 50 ppb. Without the use of acid catalyst, the array response to TATP vapor was ~ 100 times lower. Amberlyst15 decomposed TATP vapor exceptionally efficiently, and the quantity of acetone measured agreed with the stoichiometry anticipated from TATP breakdown (3:1). Amberlyst-15 is an efficient solid acid catalyst for TATP vapor breakdown since only trace quantities of TATP vapor or its decomposition products were adsorbed. Because only trace quantities of TATP vapor or its breakdown product were adsorbed, Amberlyst15 was an efficient solid acid-catalyst for TATP vapor decay.[68-70] Principal-component analysis (PCA) was used to analyze the array response at varied TATP concentrations. The connection between the total Euclidean distances of the color changes (i.e., square root of the sums of the squares of the RGB values) of the array as a function of TATP vapor concentration. The total-Euclidean distance increased monotonically when [TATP vapor] increased from 50 µg/L to 1 mg/L.[71,72]

The interaction between potassium titanyl oxalate and hydrogen peroxide (H_2O_2) produced during triacetone triperoxide degradation provides the basis for the colorimetric approach, according to Li et al. [34] To detect TATP colorimetrically, potassium titanyl oxalate could selectively react with H_2O_2 to generate an orange compound called peroxotitanic acid. All the reagents had an absorbance peak of around 200 nm. PTA exhibited an absorption peak at around 381 nm. Absorbance occurs at roughly 200 nm because of the n*-electronic transitions of Sulphur in H_2SO_4 & carbonyl in formic acid, acetic acid, acetone, & potassium titanyl oxalate (PTO). For HCl, the charge-transfer transition could be ascribed to the interaction between the Cl_2 and the H_2O molecule. TATP does not absorb UV light. PTA exhibits UV-absorption at 381 nm due to the electron transfer of the ligand's peroxyl link to Ti^{4+}. Because of the red shift in absorption, the absorbance measurements at 404 nm were observed. As the TATP content dropped, the hue got lighter. The visual observation using H_2SO_4 showed that the yellow solution was still visible even at a [TATP] 20 µg/mL. The solution became almost colorless at concentrations of 2 and 5 µg/mL. The solution's color barely changed at 10 µg/mL. In contrast, the HCl groups had comparable outcomes with varying TATP solution concentrations. The HCl group's hue was lighter than that of the H_2SO_4 group. With 60% H_2SO_4 and 30% HCl present, the lowest concentration of TATP that can be seen visually was 20 µg/mL. The absorbance in the H_2SO_4 showed

an excellent linear connection with TATP concentration, R^2 = 0.999. There was also a good linear connection in the HCl. TATP was measured in a variety of real-world samples, including tap water, river water, and soil. It implies that the spiking recoveries for TATP are in the range of 96.6%-100.8%, with a relative standard deviation (RSD) of 0.4%-4.0%.

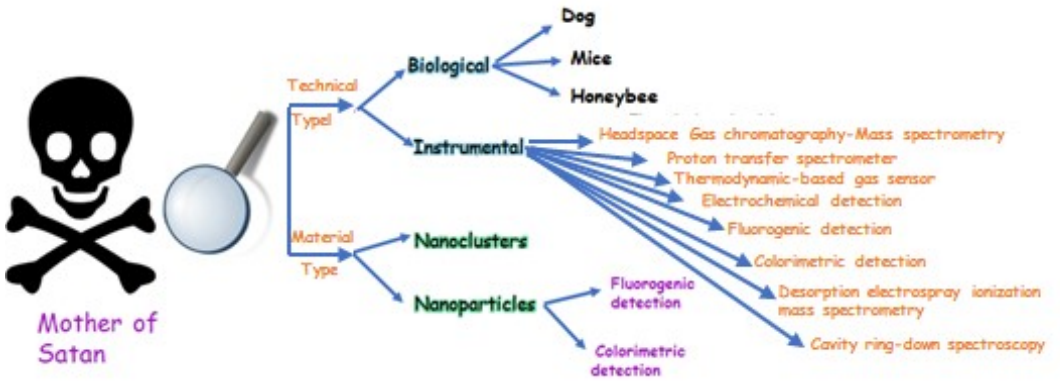

Fig. 8: Detection of TATP via different ways.

3.2 Material Type

Not only technical type techniques but also material type for TATP detection with mechanistic details are an active area of research [Fig. 8].

3.2.1 *With nanocluster*

According to Xie et al.[37] gold nanoclusters cross-link polyphenylenevinylene (PPV) derivatives with vinyl groups on the side chains to generate flexible Schottky sensors. The separation of PPV photo-generated e^-- h^+ and the intensity of photocurrent could both be promoted by collective excitation of coupled Au NCs, which in turn improves the detection sensitivity of photoelectric sensors and reduces their response time to TATP. When the feed ratios of gold nanoclusters /PPV are 1:1000, 1:800, 1:600, 1:400, 1:200, 1:100, and 1:50, respectively, the responses to TATP (defined as $(I_t - I_0/)I_0$) are 2.4, 3.8, 7.4, 11, 16.7, 81, and 32.7%, which were higher than that of pure PPV films (2.01%). The lowest TATP concentration was 50 ppb. Over repeated gas-sensing cycles, the response remains nearly constant, confirming the sensor's outstanding repeatability and stability. The maximal reaction values for the gold nanocluster/PPV films to picric acid, TNT, and DNT are 17.04, 15.96, and 7.76%, respectively. The sensor films reveal an 81% unfavorable reaction to TATP. Explosive vapours had responses of 2.17,

24.5, 2.44, and 0.91 seconds, respectively. Explosive vapours are recovered in 7.89, 9.84, 3, and 1.7 seconds, respectively. The research does not fully explain the interfacial mechanisms controlling analyte recognition and electrical response generation. It focuses on the noncontact photoelectric sensing performance of the Au nanocluster-tailored PPV Schottky sensor for TATP detection. Rather than describing the physicochemical processes taking place at the Au nanocluster/PPV contact, the discussion primarily concentrates on response magnitude and detection capabilities. Significant processes including charge separation, carrier transport, Schottky barrier modulation, and surface adsorption dynamics are still not well understood. Nanoclusters are used to increase sensing behavior, although their precise role in electron mobility, plasmonic enhancement, and active-site interaction has not been well examined. During actual usage, the suggested platform may additionally face operational difficulties due to air humidity, interfering volatile chemicals, and variations in ambient conditions. Additionally, problems with scalability for continuous field-level monitoring, calibration stability, device lifetime, and manufacturing repeatability were not fully explored.

Hosseini et al. [38] developed a thin film of polyaniline (PANI) with a nanocluster structure (CN-PANI) as a base sensor. Electrical property CN-PANI explored a convenient TATP sensor. Acetone, H_2O_2, and TATP molecules had all been detected by the sensor. TATP concentration increases, PANI and CN-PANI electrical conductivity increase, and CN-PANI results naturally improve. The electrical conductivity diminished with increasing polymer thickness, which was owing to the reduced permeability of TATP at greater thicknesses. The presence of active double bonds and differing free radical TATP (or polaron $PANI^{+}$ and bipolaron $PANI^{++}$) was thought to be the primary cause of an increase in conductivity. The electrical conductivity of PANI and CN-PANI vs time for TATP vapors at 15 ppm after 60 seconds of exposure. When an initial [TATP] of 15 ppm, the conductivity reduced quickly after removing the polymer from the vapor exposure. The conductivity did not vary with time after the first decline. When exposed to TATP, the conductivity of the CN-PANI sensor increased, indicating p-type behavior, and hence, charge transfer was mostly through the CN-PANI. The CN-PANI sensor had a reaction time that was roughly 1.5 times faster than PANI and less than 5 seconds for TATP vapor. The polyaniline nanocluster-based conductivity gas sensor's detecting effectiveness for TATP vapor analysis, but it falls short of providing a thorough explanation of the charge-interaction and molecule adsorption mechanisms causing conductivity fluctuation. Response sensitivity and detection capabilities receive more attention than the underlying mechanism that connects TATP exposure to electrical signal production. Important features include surface-induced resistance modulation, protonation–deprotonation behavior, and carrier hopping are still not well understood. Despite being used to improve analytical performance, little is known about how nanoclusters affect electron transport routes, active surface density, and interfacial contact. During real operation, the suggested sensing approach may additionally encounter difficulties due to temperature variations, humidity, and interference from volatile organic molecules. According to Hosseini et al.[38], PANI forms

a powerfully oxidizing doping intermediate complex with TATP, then interacts with another TATP or H_2O_2 molecule to generate $PANI^{++}$. Using a four-probe approach, the generated $PANI^{+}$ (polaron) and $PANI^{++}$ (bipolaron) were identified by conductivity changes. Because of the formation of p -d bonds with 2p orbitals of oxygen atoms and the electronegativity of the contributing atoms, semi-carbonyl groups in cyclic peroxides had a positive charge. Chemicals having such bands, which were found in most peroxides, dangerous compounds such as TATP, were expected to alter the electrical properties of PANI films via a p-doping or oxidative process. PANI films had a significant influence on the cyclic TATP molecule.

$$(TATP) \text{ or } (PANI)^{+o}\ (PANI)^{+} \longrightarrow PANI + TATP \text{ or } H_2O_2 \ldots\ldots(1)$$

3.3.2 *With Ions*

Thermal breakdown using a iron (II) promoted method

A visual colorimetric technique for on site and quick sensing of TATP based on the iron (II) assisted heat breakdown procedure of TATP was disclosed by Zhang et al.[41] The inert 3,3′,5,5′-tetramethylbenzidine (TMB) is oxidized by the subsequent hydroxyl and Fe (III) to produce the pale-yellow oxidized product (oxTMB). The current colorimetric assay for TATP uses the TATP-Fe^{2+}-TMB ternary chromogenic system and has a dynamic range of 0.5 to 30 µM with a LOD of 0.13 µM. Furthermore, ordinary compounds (such as inorganic salts, tiny organic molecules, and polymers) did not affect TATP sensing. The visual colorimetric sensing effectiveness of TATP by Fe(II)-promoted thermal breakdown, but it falls short of providing a thorough explanation of the molecular-level mechanisms behind chromatic response production and analyte identification. While offering little insight into the thermally induced breakdown process and subsequent chemical changes, the discussion mostly concentrates on detection capabilities and visual signal creation. Crucial elements impacting the optical response, such as radical production, electron-transfer behavior, and Fe(II)-mediated catalytic activity, are still not well understood. The role of nanoscale materials to catalytic acceleration, surface contact, and signal stabilization is not well investigated, despite the demonstration of improved analytical performance. During real operation, oxidizing pollutants, temperature changes, and ambient humidity can potentially interfere with the sensing strategy. Zhang et al.[41] showed TATP could be degraded into H_2O_2 when heated, and it interacts with iron(II) to form OH radical and iron (III) via the Fenton reaction [Fig. 9].

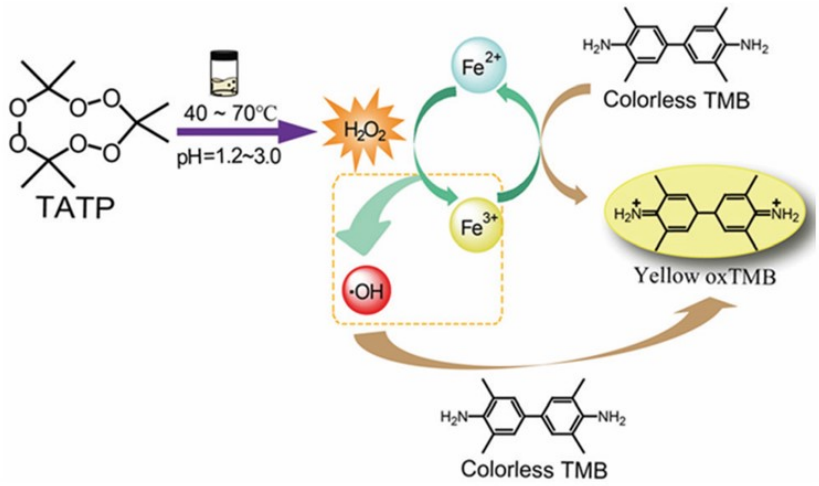

Fig.9: Schematic of the visual colorimetric assay for TATP based on the Fe(II)-promoted thermal decomposition process. (reprinted with permission Zhang et al.[41])

3.2.3 *With nanoparticles*

3.2.3.1 Current variation

With the help of cyclic voltammetry (CV) and electrochemical alteration of the glassy carbon (GC) electrode with peroxide-based explosives (PBE)-memory polycarbazole (PCz) films embellished with gold-NPs, according to Saglam et al.[39] An electrochemical detector for the sensitive and selective measurement of peroxide-based explosives such as TATP and HMTD. An oxidation peak of 1.27 V, a reduction peak for PCz of 0.781 V, and a reduction peak for TATP of 1.081 V were all produced by the TATP-memory GC/PCz electrode. These peaks resulted from the radical oxidation of the monomer cation. The quantity of monomer and TATP in the solution mixture dropped as the number of cycles grew, while the quantity of polymer and TATP deposited on the electrode surface rose. In the first cycle of gold nanoparticles deposition on the TATP-memory-GC/PCz-adapted electrode surface. Au^{3+} reduction to gold nanoparticles was found at about -0.28 V. Because trivalent gold was transformed to AuNPs and deposited on the electrode surface, the current due to the residual Au^{3+} ions decreased as the number of cycles increased. After a certain number of cycles (40), the intensity of current due to Au^{3+} ions does not change, suggesting that the maximum quantity of gold nanoparticles that could gather on the electrode surface was obtained. By detecting cathodic peak currents, the electrochemical detector electrodes worked well for direct TATP detection in an attentiveness range of 0.1- 1mg L^{-1} with a LOD of 15 µg L^{-1}. The polycarbazole/gold nanoparticle-modified glassy carbon electrode's electrochemical sensing efficiency for the direct detection of TATP and HMTD does not fully account for the molecular imprinting interactions that lead to selective analyte binding. While offering a limited understanding of the electron-transfer processes controlling signal creation, the discussion mostly

concentrates on analytical response and sensitivity. Crucial mechanisms including charge transfer across the conductive matrix, cavity–analyte affinity, and interfacial adsorption behavior are still not well understood. Although gold nanoparticles are added to boost sensing performance, their contribution to surface-active site creation, conductivity improvement, and catalytic enhancement is not well examined. During actual use, the suggested sensing platform may potentially run into issues with competing peroxide species, electrode fouling, and environmental changes. During actual use, the suggested sensing platform may potentially run into issues with competing peroxide species, electrode fouling, and environmental changes. Additionally, factors pertaining to mobility for real-time field applications, calibration consistency, long-term electrode stability, and manufacturing repeatability were not fully examined. During actual use, the suggested sensing platform may potentially run into issues with competing peroxide species, electrode fouling, and environmental changes. Additionally, factors pertaining to mobility for real-time field applications, calibration consistency, long-term electrode stability, and manufacturing repeatability were not fully examined. TATP and HMTD electrochemical analysis is often done indirectly (by converting their bound peroxides into H_2O_2 under proper circumstances). The developed method relies on the formation of H-bonds between the hydrogen atom of the NH group in the carbazole units of the polymer and the oxygen atom in the peroxide (C-O-O-C) bonds of TATP and HMTD molecules [Fig. 10].

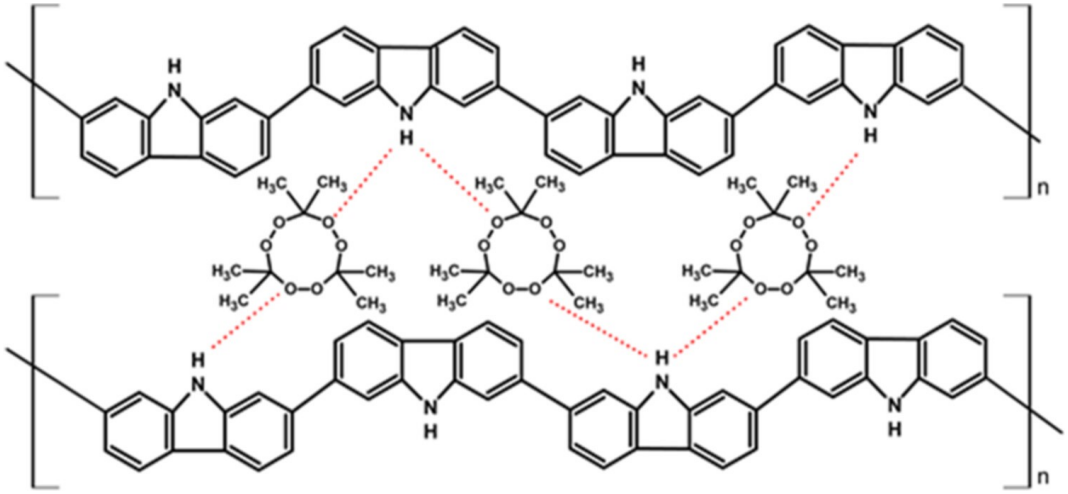

Fig. 10: TATP-PCz Hydrogen Bond Formation Mechanism (reprinted with permission Saglam et al.[39]).

3.2.3.2 Colorimetric Sensing

With titanium oxide nanoparticles

For the detection of H_2O_2 and TATP, Gökdere et al.[40] created two unique titanium dioxide nanoparticle-based visualization sensors based on compound creation on the solid surface. The one-sensor, a paper sensor based on (3-aminopropyl)triethoxysilane (APTES) modified TiO_2NPs (APTES@ titanium dioxide nanoparticles), takes use of peroxo-titanate double compound production among APTES@ titanium dioxide nanoparticles & hydrogen peroxide on chromatographical paper. The second sensor, a 4-(2-pyridylazo)-resorcinol-adapted titanium dioxide nanoparticles-based solid sensor (PAR@ titanium dioxide nanoparticles), was based on the production of a ternary compound among Titanium (IV), PAR, and hydrogen peroxide. After samples had been hydrolysed in acid to produce hydrogen peroxide, TATP was also measured using the existing detectors. The synthesised TATP's mass spectrum was examined using gas chromatography-mass spectrometry. At SIM mode, the analyte created a characteristic ion with a (mass/charge) value of 43. The TiO_2NPs-based detection methods developed were based on acid-hydrolysis of TATP into hydrogen peroxide, pH alteration to 7, and distinct application of titanium oxide nanoparticles-based detectors to this medium to create two peroxotitanate and 3 titanium (IV) PAR H_2O_2 complexes of H_2O_2 using APTES@TiO_2NPs and PAR@TiO_2NPs. The calibration curve developed from the APTES@TiO_2NPs-based paper sensor when applied to H_2O_2 solutions (generated from the hydrolysis of TATP) at [1.25×10^{-3} - 1.25×10^{-1} M].

$$R= 4.24 \log C_{TATP} + 14.94 \ (r^2 =0.9986)$$

where C_{TATP} was the solution's [TATP] (in M) and R was the reflectance value (%). The paper-based APTES@ titanium dioxide nanoparticle sensor's LOD was 5.13×10^{-4} mol/L. The calibration curve from a solid sensor based on PAR@ titanium dioxide nanoparticle when used with hydrogen peroxide solutions among [3.25×10^{-6} and 3.25×10^{-2} M].

$$R= 5.12 \log C_{TATP} + 32.04 \ (r^2 =0.9993)$$

The (LOD) of a solid sensor based on PAR@ titanium dioxide nanoparticle was 3.54×10^{-7} mol L^{-1}.

The TiO_2NPs-based solid sensor was demonstrated by Gökdere et al.[40] to be more sensitive to H_2O_2 and TATP than most analogous reduction-oxidation reactions of H_2O_2. It took advantage of the creation

of a ternary complex between titanium dioxide, H_2O_2, and PAR. Such 3-complexes give superior sensitivity and selectivity (than 2-complexes) to analytical results. Titanium dioxide nanoparticles' colorimetric sensing capabilities for identifying TATP and hydrogen peroxide, however, do not fully explain the chemical mechanisms behind analyte interaction and optical signal production. The photocatalytic and surface-chemical processes controlling response production is less important than sensitivity and apparent color fluctuation. Significant elements including the creation of electron–hole pairs, the participation of reactive oxygen species, and spectrum alterations brought on by adsorption are still not well understood. TiO_2 nanoparticles are used to improve analytical behavior, but they affect surface reactivity, charge separation efficiency, and catalytic activation. During real operation, oxidizing chemicals, humidity variations, and ambient light conditions may potentially interfere with the suggested approach. Additionally, issues with long-term stability, flexibility for portable real-time applications, quantitative accuracy, and sensor reusability were not fully assessed.

With Silver Nanoparticles

Uzer et al.[42] demonstrated the use of silver nanoparticles to create a colorimetric H_2O_2 and TATP sensor. They demonstrated that the analyte (H_2O_2) selectively oxidized silver nanoparticles to silver (I), which then selectively oxidized the tetramethylbenzidine to a blue coloured diimine. The detector was optimized for quantifying H_2O_2 and TATP (linear correlation 0.9997) at 655 nm. TATP was easily measured in the field since it was easily hydrolyzed to H_2O_2 with a strongly acidic cation exchange resin, with a LOD was 0.31 mg L^{-1}. The "turn-on" colorimetric sensing capabilities of silver nanoparticles for TATP and hydrogen peroxide detection, but it does not fully explain the molecular processes behind analyte identification and optical signal development. Instead of describing the redox-mediated mechanisms governing nanoparticle aggregation and color transformation, the talk mostly concentrates on sensitivity and observable response production. Significant phenomena including electron-transfer routes, surface plasmon resonance modulation, and catalytic oxidation behavior are still not well understood. Although silver nanostructures are used to enhance analytical performance, little is known about how they affect surface reactivity, adsorption efficiency, and signal amplification. Under real-world circumstances, oxidizing pollutants, humidity fluctuations, and colloidal nanoparticle instability may potentially interfere with the sensing technique.

Using Fe_3O_4 Magnetic Nanoparticles on Nafion with N, N-Dimethyl-p-phenylenediamine (DMPD) Sensor

Can et al.[43] demonstrated DMPD-TATP-iron oxide magnetic nanoparticles absorption spectra and TATP-DMPD absorption spectra (40 mg/L TATP). At 100-fold concentrations of TATP, common ions present in soil & groundwater [potassium (I), magnesium (II), calcium (II), chloride (I), nitrate (I), sulfate (II)] had little effect on recovery in both solutions (96-104 %) and Nafion membrane applications (97- 108 %). TATP working solutions in acetone at attentiveness ranging from 1 to 10.00 mg L^{-1} were analyzed by gas chromatography-mass

spectroscopy and the mean value of 3- repeated insertion was utilized for each computation.[73] The calibration equation for peak area (A) and attentiveness was developed against GC-MS method. The sensing capabilities of the N,N-dimethyl-p-phenylenediamine/Nafion platform using Fe_3O_4 magnetic nanoparticles for TATP measurement, but it doesn't fully explain the chemical interactions that lead to signal creation and analyte identification. Clarifying the oxidation-reduction mechanisms influencing color or electrical change is less important than analytical sensitivity and response behavior. Significant processes including surface adsorption kinetics, magnetic nanoparticle-assisted charge transfer, and catalytic electron exchange are still poorly understood. Fe_3O_4 nanostructures are used to increase sensing efficiency, although their role in active-site formation, conductivity augmentation, and interfacial stability has not been well studied. During real operation, oxidative interferents, ambient humidity, and matrix contamination may potentially cause problems for the suggested approach.

$$A = 4.17x10^4C_{TATP}-1.10x10^4 \ (r = 0.9998)$$

According to final attentiveness (DMPD with ROS)

$$A_{554\ nm} = (9.48\pm0.48)\ x10^{-2}C_{TATP} + (7.40\pm2.93)\ x10^{-2}$$

TATP (r^2= 0.9993)

where the molar absorptivity for TATP was $\varepsilon = (21.06\pm1.07)\ x\ 10^3$ L mol^1 cm^{-1} , LOD = 0.47 mg/L , LOQ = 1.57 mg/L.

The strategy put out by Can et al.[43] was found on the acidic hydrolysis of TATP into hydrogen peroxide, pH was 3.7, and the accumulation of iron oxide magnetic NPs in this medium to yield ROS (i.e. hydroxyl and perhydroxyl radicals) from hydrogen peroxide. For more accurate spectrophotometric detection of this coloured product in solution or on a Nafion-membrane, the new ROS oxidises DMPD to produce the coloured $DMPD^+$ radical cation [Fig. 11].

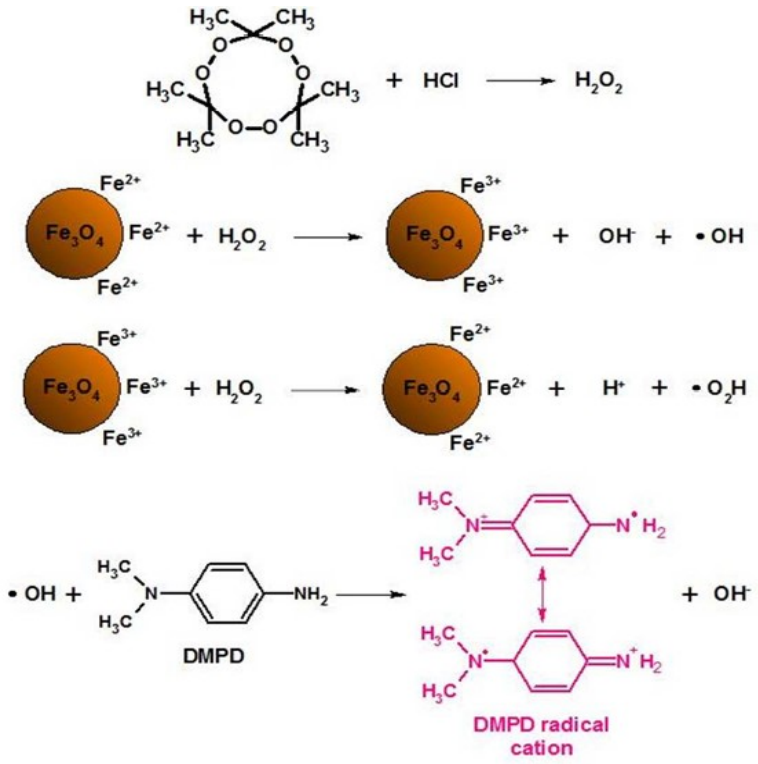

Fig. 11: Diagram depicting TATP hydrolysis, H_2O_2 creation, ROS generation, and $DMPD^+$ radical cation formation for indirect spectrophotometric TATP detection (reprinted with permission Can et al.[43]).

With Ag@ZnMOF composite

A sensitive probe for the sensing of H_2O_2-based EP was observed by Bagheri et al.[44] based on the peroxidase-mimic activity of a Ag@Zn flake-like MOF compound (Ag@ZnMOF). The template analyte, TATP, was broken down into H_2O_2 under acidic conditions. The final solution's absorbance (at 652 nm) and [TATP] were calibrated linearly, and the range of the arc was from 0.4 to 15.0 mg/L ($A=0.098\ C(TATP) + 0.075$, $R^2=0.999$). The 0.10 mg L^{-1} detection limit was chosen. The values of RSD% were found to be 2.93 and 3.48, respectively.[74] The study primarily focuses on the Ag @ZnMOF nanocomposite's visual sensing capabilities for peroxide-based explosive detection; however, it does not provide a thorough explanation of the molecular-level interactions that underlie analyte identification and chromatic signal production. The catalytic and electrical mechanisms controlling signal formation are largely ignored in favor of focusing on detection sensitivity and visual color response. Significant processes include MOF-assisted diffusion paths, adsorption-driven electron transfer, and surface plasmon modulation are still poorly understood. While the Ag@ZnMOF hybrid structure is intended to improve analytical efficiency, the nanocomposite's precise role in active-site accessibility, catalytic activity, and response amplification has not been thoroughly examined. Under

real-world environmental circumstances, oxidizing interferents, air moisture, and structure instability may potentially cause problems for the suggested sensing method. Moreover, problems with quantitative precision, long-term operational durability, manufacturing repeatability, and adaptation for portable field-level monitoring were not fully investigated. Peroxidase-like catalyst's mechanisms were defined based on their capacity to break down H_2O_2 to free •OH. To demonstrate Ag@ZnMOF's improved impact on H_2O_2 breakdown and production of additional •OH, terephthalic acid was used as a 2-peroxidase substrate, which can selectively be reacted with •OH to create luminescent 2-hydroxyterephthalic acid emitting at 425 nm (λ_{ex} = 315 nm). An auspicious mimetic effect was established for a newly produced Ag@ZnMOF nano-composite using this method. A 500 µL insertion of tert-butanol might entirely prevent the formation of the blue color. As a result, the primary involvement of •OH in the catalytic oxidation of 3,3′,5,5′-tetramethylbenzidine was established.[44]

In order to determine TATP directly, a molecular spectroscopic sensor was created based on the hydrolysis of TATP without the use of exogenous acid. Utilizing TATP's solubility in acetone, the developed sensor's detection principle relies on the breakdown of TATP by hydrochloric acid, which is produced when TATP reacts with hydroxylamine hydrochloride, and hydrogen peroxide, which is produced as a degradation product to form hydroxyl radicals catalyzed by goethite nanoparticles. Because of their potent oxidation capabilities, the generated hydroxyl radicals converted N,N-dimethyl-p-phenylenediamine (DMPD) to the pink-hued $DMPD^{\bullet+}$ radical cation. The absorbance of the resulting colored product was used to determine TATP directly. The devised method was applied to TATP samples produced in acetone, and the results were evaluated by measuring the absorbances caused by $DMPD^{\bullet+}$ at 554 nm. Within the final range of 10–33 mg L^{-1}, a calibration curve was made between absorbance and TATP concentration. The developed TATP technique has a limit of quantification (LOQ) of 10.8 mg L^{-1} and a limit of detection (LOD) of 3.3 mg L^{-1}. The relative standard deviations (RSD%) for TATP were determined to be 2.70% and 3.76%, respectively, after five repeat measurements were carried out to assess the intra-assay and inter-assay precision of the spectrophotometric detection of TATP.[75]

3.2.3.3 *Fluorogenic sensing with TATP*

Turn on-off-on" sensing with Hg^{2+} and TATP

Tawfik et al.[76] demonstrated the concept of an on/off/on detection system for Hg^{2+} and Triacetone triperoxide**,** in which polythiophene-coated (PQD) emission was efficiently quenched after the accumulation of Hg^{2+} but significantly restored with the accumulation of TATP. The influence of pH on the recovery of TATP luminescence on the constructed polythiophene-coated Hg^{2+} probe was

investigated over the range from 4 to 11. At pH 7.0, the highest recovery of fluorescence emission was attained. This might be because too extreme or too little a pH disrupts the complexation and decreases the affinity between Hg^{2+} and TATP. The optimum response time for Hg^{2+} detection is within 10 min, while for TATP detection it is within 5 minutes. TATP might be used to reestablish the emission of the polythiophene-coated Hg^{2+} compounds.[77,81] This retrieval did not appear to happen when other readily accessible explosives such as trinitrophenol (TNP), dinitrophenol (DNP), p-nitrophenol (PNP), and C_6H_5OH (500 mg/L^{-1}) were added. After 50 mg/L^{-1} of TATP was added to the PQD-Hg^{2+} scheme, the unexpectedly selective luminescence switch-off then switch-on response was detected. The PQD-Hg^{2+} demonstrated unique selectivity for TATP by increasing the intensity while interacting with none of the other explosives.[79,80]

The luminescence intensity at 510 nm rose as TATP content increased. As the concentration of TATP rose, the emission intensity progressively recovered. With a correlation coefficient of 0.995, the value of (F/F_0) rapidly rose, a substantially linear connection (range from 2.5 to 50 mg/mL^{-1}) with the [TATP]. The LOD for TATP was 0.055 mg L^{-1} (RSD ~1.0). The "on-off-on" sensing system for Hg^{2+} and TATP successfully quenches PQD emission after Hg^{2+} addition but significantly recovers with TATP addition. Fluorescent sensors can cause entangled intramolecular charge transfer. The photo-induced electron transfer (PET) process has been used to construct metal transfer sensors. Probes often rely on the well-known quenching effect of amines caused by PET. Hg^{2+} may significantly reduce QD emission by eliminating non-radiative electron/hole recombination through efficient electron transfer mechanisms. The mechanism is as follows: adding Hg^{2+} greatly reduces the emission of PQDs, whereas TATP restores the fluorescence. UV light caused excited QDs to revert to their ground state and emit brilliant green light. Quenching is caused by electron transport. When Hg^{2+} was added to the PQD solution, it reacted with the amino and carboxyl groups on the surface, transferring electrons from the excited PQDs to the unoccupied d-orbitals of Hg^{2+}. This caused the PQDs' emission to decrease. When TATP was added to the PQD-Hg^{2+} system, it enhanced the interaction between Hg^{2+} and TATP, resulting in the release of the free dyad and restoration of emission. The greater binding force between TATP and Hg^{2+} led to the synthesis of $[TATP\text{-}Hg]^{2+}$, allowing for emission recovery [Fig. 12].

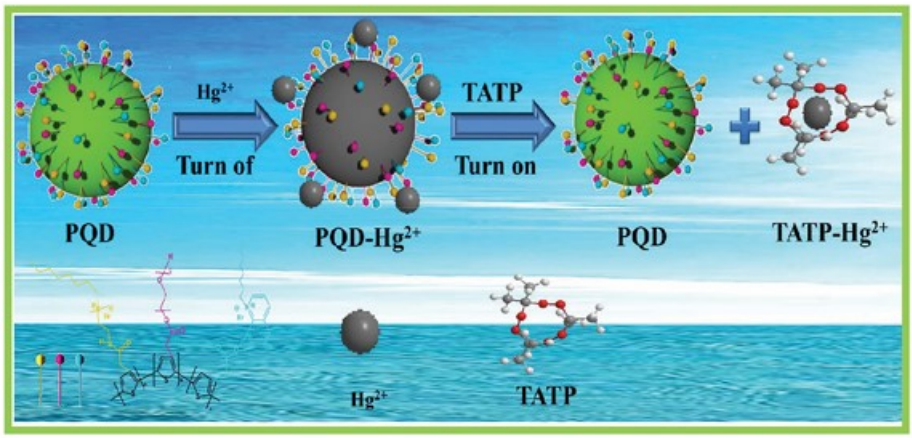

Fig,12: On–off–on" detection mechanism of Hg^{2+} and TATP based on conjugated polythiophene-QD nanohybrid materials. (reprinted with permission Tawfik et al.[76]).

Tawfik et al.[76] discovered that adding Hg^{2+} greatly reduced the emission of polythiophene-coated, but that adding TATP reinstated the fluorescence. When exposed to UV-visible radiation, the excited quantum dots reverted to their ground state, emitting brilliant greenish light. The quenching method was thought to be caused by electron transfer. After adding Hg^{2+} to the polythiophene-coated solution, the Hg^{2+} reacted with the amino. COOH group on the emergence of the polythiophene-coated, resulting in electron transfer from the polythiophene-coated to the unoccupied d-orbitals of Hg^{2+}, quenching the polythiophene-coated emission. TATP was injected into the polythiophene-coated Hg^{2+} system. Hg^{2+} was free from the scheme due to the greater interaction between Hg^{2+} and TATP. The presence of Hg^{2+} had a significant quenching impact on PQDs through processes inherent to paramagnetic species, which could operate as slackers via the electron transfer procedure. When the potent oxidizing agent TATP was added, the Hg^{2+} ions were merely detached from the surface of the polythiophene coating by forming a metal chelate compound with TATP.

With Silica nanomaterial

Fluorogenic silica nanoparticles were developed by Garcia-Calvo et al.[45] to produce fluorescence when exposed to TATP vapours. Perylenemonoimides and Perylenediimides (PMIs/PDIs) containing a single p-aminopyridyl group were created to show their suitability and sensitivity to oxidants. PMIs/PDIs having one p-aminopyridyl group, to study their suitable characteristics and sensitivity to oxidants and their covalent anchoring to silica materials having a protective N-Boc group JG125/PC63, the unprotected compounds JG125d/PC63d, obtained by acidic deprotection, and the functionalized

triethoxysilyl derivatives JG131/JG135. In certain common organic solvents, the purple complexes JG125/JG125d or PC63/PC63d fluoresced sporadically. Through changes in turn-on fluorescence, JG125 and PC63 were very sensitive to TATP. They obtained an increment in QY from φ_{JG125} (chloroform) =0.23 $\pm$ 0.01 to $\varphi_{JG125+TATP}$ (chloroform) 0.65 $\pm$ 0.01 in the presence of TATP, with an overall rise of $\varphi_{JG125+TATP}/\varphi_{JG125}$ =2.8. The LOD was 620 µM [0.11 mg/mL] for TATP. For PC63 (2.5 µM, λ_{exc} = 484 nm, λ_{em} = 336 nm), QY from φ_{PC63} (chloroform) = 0.27 $\pm$ 0.01 to $\varphi_{PC63+TATP}$ (chloroform) = 0.36$\pm$ 0.01, and a inferior total increment of $_{\varphi PC63+TATP}/\varphi_{PC63}$ =1.3. The LOD for TATP was 4.83 µM [0.84 mg/mL]. Therefore, for nJG131 the total increment of the QY in the existence of TATP-vapor was $\varphi_{nJG131+TATP}/\varphi_{nJG131}$ = 3.5 and for nJG135 the total increment of the QY in the existence of TATP-vapor was $\varphi_{nJG135+TATP}/\varphi_{nJG131}$ = 3.1, the total increment of the QY in the existence of HCl vapor was considerably inferior, $\varphi_{nJG131+HCl}/\varphi_{nJG131}$ = $\varphi_{nJG135+HCl}/\varphi_{nJG131}$ =1.6. The increment in fluorescence in the presence of TATP vapor was adequate in all cases for meaningful measurements. They showed that the fluorescent reaction of the resources to the existence of TATP was enduring, allowing it to be evaluated at any time after the TATP elucidation. According to an analysis of the E-field intensity distribution, creating homojunction between the urchin-shaped titanium-oxide nano-sphere & titanium oxide nano-arrays could increase the localised electromagnetic field at the interface of junctions, which might provide photocatalytic active sites to diminish TATP molecule by encouraging charge severance.

Garca-Calvo et al.[45] showed the photoelectrons gather at the homojunction's interface, providing an active site for photocatalysis to convert TATP into acetone and hydrogen peroxide. An amino-replaced C_5H_5N-side group was oxidized as part of the procedure, quenching the attached fluorophore's luminescence by an intra-molecular charge-transfer action until it was oxidized, releasing the original luminescence of the (PMIs/PDIs) fluorophores.

The portable testing apparatus for the identification of triacetone triperoxide (TATP), a frequent element in homemade explosives, was described by Revilla- Cuesta et al.[81] By merely circulating air samples through the detecting mechanism beneath the air conditioning system of a typical room, the device enables field testing and the creation of real-time findings to test for TATP vapor traces in air. Thus, the regulated trapping of the analyte in the chemical sensor provides accurate findings at very low concentrations of TATP in air under real-life settings, making it appropriate for everyday usage in airline luggage storage or a locker room at a big sporting event. By comparing the material's fluorescence before and after exposure to TATP traces in air, the highly sensitive and selective fluorescent methodology enables the trapping of triacetone triperoxide in the chemical sensor to provide dependable results at very low concentrations in air under ambient conditions. The silica nanoparticle/fluorescent dye assembly's ultrasensitive detection capability for airborne TATP sensing, however it does not methodically describe the intricate process of interaction between TATP molecules

and the fluorescent recognition unit. The fundamental signal conversion processes that cause fluorescence amplification or quenching are very briefly discussed in the paper, which mainly focuses on fluorescence response and detection sensitivity. The internal mechanisms pertaining to surface contact, charge transfer, energy transfer, and fluorescence amplification are not well examined, despite the fact that silica nanoparticles are employed to increase sensing efficiency. Additionally, it is yet unclear the nanomaterials affect signal stability, molecule confinement, and adsorption capacity. Further practical drawbacks of the testing procedure include reliance on controlled laboratory settings, potential interference from ambient vapors, susceptibility to humidity, and difficulties in maintaining consistency during real-time airborne detection. Furthermore, problems with continuous field monitoring, mobility, large-scale deployment, and long-term sensor stability were not fully addressed.

With Carbon dots

Koc et al.[82] creating a novel method for the first-ever direct measurement of intact triacetone triperoxide (TATP). A microwave-assisted approach was used to create carbon quantum dots doped with nitrogen and oxygen (APT-CDs; Ascorbic acid-Polyethyleneimine-Triethylenetetramine Carbon quantum Dots) with a high quantum yield (66.8%). In the presence of acetone, photoinduced electron transfer (PET) and hydrogen-bonding processes suppress the blue fluorescence of APT-CDs. A considerable amount of the original fluorescence may be restored by adding intact TATP in the crucial concentration range to an acetone solution of APT-CDs at quenched fluorescence. Spectrofluorometry and smartphone applications can be used to track the regained fluorescence. Because of noncovalent interactions with acetone molecules that bind (by H-bonding) with APT-CDs at ground-state, TATP creates molecular aggregates that prevent a certain portion of acetone molecules from interacting with carbon dots. The TATP detection limit (LOD) offered by this approach is 0.18 nmol l^{-1} (0.75 nmol l^{-1} for smartphone applications). TATP determination has good recoveries (94.2%–105.7%), and it is not significantly impacted by potential interferers.[79]

Koc et al.[83] suggest a Cu(I)-driven Fenton-like reaction to determine TATP simultaneously using colorimetric and fluorometric methods in the same reaction tube. CuI, a precursor metal cation that has to be acidic, oxygen- and nitrogen-doped carbon dots (ascorbic acid-urea-carbon dots) (AU-CDots), the color reagent N,N-dimethyl-p-phenylenediamine (DMPD), and TATP are all included in the same reaction tube as the analytical apparatus. TATP is hydrolyzed by the hydrochloric acid needed to dissolve CuI, and the hydrolysate H_2O_2 then reacts with CuI in a Fenton-like manner to produce CuII and hydroxyl radical (•OH). While •OH interacts with DMPD to produce a colorful radical cation ($DMPD^{\bullet+}$), the resultant CuII preferentially interacts with the AU–CDots to extinguish fluorescence. TATP can therefore be measured concurrently using colorimetric and fluorometric techniques. For the

fluorometric and colorimetric tests, the approach yields a TATP detection limit (LOD) of 3.0 nmol L^{-1} and 10.0 nmol L^{-1}, respectively.

Abajo-Cuadrado et al.[84] report a multilayer fluorogenic material that is used on a mechanized apparatus for semi-autonomous measurements of airborne triacetone triperoxide (TATP) in operating areas. It consists of a fluorescent probe mounted on silica, polydimethylsiloxane, and glass slides. They had built the first semiautonomous airborne TATP detection system that is useful for scanning the presence of IEDs in everyday environments by utilizing a UV LED and a commercial micro-fluorometer as the measuring block, a mini-PC and a Wi-Fi card as the control block, all integrated in a mobile robotic platform, and a mobile phone as the receiver. It operated by exposing a sensor stick to the room's air flow and transmitting the distant measurements to an app on a smartphone.[84]

4. Spot Analysis

An et al.[59] showed that a practical analytical strategy has offered an alluring alternative since it is simple to recognize changes in color and brightness. When TATP vapor was immediately quenched after being inserted onto the luminescent paper's surface, the color changed from pink-purple under UV light [Fig. 13].

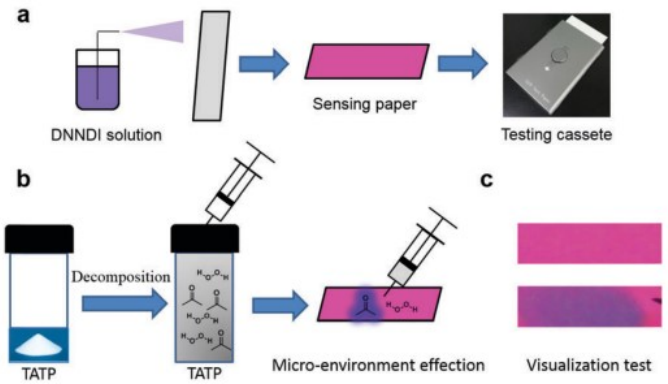

Fig. 13:(a) TATP testing cassette template; (b) TATP vapor sensing mechanism; (c) TATP vapor visualization test (reprinted with permission Can et al.[43]).

Li et al.[34] demonstrated the color lightened as the TATP content decreased. The visible yellow solution could still be found in the experimental group with H_2SO_4 when the quantity of TATP twenty g/millilitre was as less as. When the attentiveness was between two and 5 g/mL, the solution was practically colourless. When the attentiveness was 10 µg/mL, the color of the solution changed insignificantly. Under varied amounts of TATP solution, the hydrochloric groups produced comparable findings. The colour of the HCl group, however, was light when compared to the H_2SO_4 group. The minimal concentration of TATP was detectable by eye inspection under the conditions of 60% H_2SO_4 and 30% HCl was determined to be 20 µg/mL.

Due on the colorimetric TMB-H_2O_2-Ag@zincMOF system, Bagheri et al.[44] developed an easy-to-use and sensitive method for the real-time detection of TATP, a dangerous & crucial analyte. TATP was first added to the TMB-Ag@ZnMOF solution and then oxidised to H_2O_2 in a moderately acidic medium. Ag@ZnMOF caused H_2O_2 to oxidize TMB, which creates the blue-oxTMB product. The solution's absorbance intensity at six-hundred-fifty-two nanometres, which was inversely proportional to the TATP content, served as the detection signal.

Can et al.[43] demonstrated the characteristics of Nafion membranes (earlier and afterward treatment of TATP samples at various concentrations after hydrolysis to hydrogen peroxide), showing that the original membrane altered colour from light red-pink to dusky red-pink in the presence of hydrogen peroxide formed from dissimilar [TATP].

5. Real Water Analysis

Li et al.[34] demonstrated real water sampling for TATP detection. The current approach yielded spiking recoveries for TATP that fell within the range of 96.6% to 100.8%, and the relative standard deviation (RSD) was determined to be 0% to 4 %. This study's findings provide evidence that the procedure devised was reliable and accurate to a high degree. It will demonstrate promising results when subjected to the TATP analytical procedure on actual samples [Table 3]

Table 3: Recovery of TATP in real water samples. reproduced from the open access publication.[34]

Sample	Added (μg/mL)	Measured by this method (μg/mL)	Recovery by this method (%)	RSD (%)
Tap water	50	48.6	97.3	2.7
	100	100.2	100.2	0.4
	200	199.0	99.5	1.1
River water	50	48.6	97.3	2.4
	100	100.9	100.9	1.2
	200	199.0	99.5	1.1
Soil	50	48.3	96.6	4.0
	100	99.9	100.0	1.4
	200	199.9	100.0	0.6

By analysing spiked aquatic samples (2-stream samples obtained from the suburbs of Tabriz & 1-under-ground aquatic sample received from East-Azarbaijan-Regional-Water Co.), Bagheri et al.[44] proved procedure validity. Additionally, it was applied to evaluate TATP in spiked real samples to investigate the reliability of the suggested portable test kit. TATP was added to three water samples at varying concentrations (0.2, 2, and 10 mg L^{-1}), and the samples were then subjected to prepared assays for analysis [Table 4].

Table 4: TMB-Ag@ZnMOF system was used to colorimetrically determine TATP in spiked water samples and soil sample, compared to the approved GC-MS method.reproduced from the open access publication.[44]

Sample	Added) mg L-1	Found (GC-MS)	Found (colorimetric method)	Recovery % ± RSD	t-statistic
River water	2.0	1.96±0.03	1.94±0.05	96.80±2.52	1.23
	5.0	4.90±0.03	4.86±0.08	97.11±1.73	2.34
	8.0	7.92±0.16	8.17±0.19	102.14±2.29	2.78
Underground water	2.0	1.95±0.02	1.97±0.04	98.30±2.22	1.59
	5.0	4.86±0.03	4.82±0.04	96.41±0.90	2.12
	8.0	7.78±0.04	7.84±0.14	97.96±1.83	2.34
River water	2.0	1.95±0.05	2.02±0.05	100.88±2.59	2.44
	5.0	4.88±0.10	4.90±0.12	96.06±2.53	1.37
	8.0	7.85±0.13	7.72±0.21	96.48±2.71	1.68

Sample	Added (mg g^{-1})	Found (GC-MS)	Found (colorimetric method)	Recovery % ± RSD	t-statistic
Soil sample	0	5.64±0.23	5.55±0.13	-	1.18
	5	10.50±0.18	10.59±0.33	97.27±3.62	0.46

The concentrations of Hg^{2+} and TATP in ambient water samples (tap & stream) that had been diluted fifty times and spiked with 3-dissimilar quantities of [Hg^{2+}] (1.0, 5.0, and 10 M) and TATP (0.076, 0.76, and 7.6 mg/L) were studied by Tawfik et al.[76] With RSDs of less than 5.0% for Hg^{2+} and TATP ranging from eighty-eight to hundred percent for tap-water and 91 to 124 % for river water, the recoveries were good.

6. Conclusions and Future Outlook

Advancements in explosive detection have become increasingly essential, driven by the urgent needs of homeland security and demining operations. Luminous materials—used in electronics, imaging, and sensor systems—hold great potential for detecting real-world threats like buried landmines or soil and groundwater contamination. Although fluorescent probes have achieved impressive sensitivity in detecting nitroaromatic compounds (NACs), reaching tolerable detection limits, it remains uncertain whether these techniques can directly sense vapors of actual explosives such as TNT, DNT, or TATP from packed bombs or landmines in real environments.

Current field methods predominantly rely on detecting more volatile taggants like DMNB rather than the explosive substances themselves. DMNB is added to plastic explosives precisely because its higher vapor pressure makes it easier to detect. Lab studies have successfully used nanoporous silica for preconcentration, capturing DMNB vapor before thermal desorption into GC–MS systems, but these have not yet translated into broadly deployed field sensors capable of sampling actual explosive vapors.

Looking forward, research must pivot from controlled lab conditions to practical application environments—such as minefields, traffic hubs, and border crossings. Of critical importance is achieving standoff detection: identifying explosive vapor from a safe distance. This is made exceedingly difficult by the extremely low vapor pressures of explosives and their rapid dilution as distance increases, which also elevates the likelihood of false alarms. Consequently, systems must be capable of both efficient vapor collection and robust preconcentration to ensure an adequate number of explosive molecules can be detected within a reasonable timeframe. In summary, developing effective field-ready sensors hinges on integrating three core capabilities: sensitive fluorescent detection, high-efficiency sample collection, and preconcentration, especially for actual explosive compounds rather than taggants. These advanced sensor technologies can transition from promising laboratory demonstrations to dependable real-world applications only by overcoming these challenges.

Conflicts of interest

There are no conflicts to declare.

Consent to Participate

All the participants checked the paper and have consent for the submission.

Consent to Publish

All the participants consented to publish.

Authors Contributions

Priyanka Sharma - Writing – original draft

Mainak Ganguly- Writing – review & editing; Supervision

Ankita Doi - Writing – review & editing

Mamta Sahu - Writing – review & editing

Funding

We have no funding to disclose.

Competing Interests

There is no competing interest to disclose.

Availability of data and materials

The data and materials are publishable free of cost.

References:

1. X. Sun, Y. Wang and Y. Lei, Chemical Society Reviews, 2015, 44, 8019-8061.
2. M. E. Germain and M. J. Knapp, Chemical Society Reviews, 2009, 38, 2543-2555.
3. Y. Salinas, R. Martínez-Máñez, M. D. Marcos, F. Sancenón, A. M. Costero, M. Parra and S. Gil, Chemical Society Reviews, 2012, 41, 1261-1296.
4. H. Östmark, S. Wallin and H. G. Ang, Propellants, Explosives, Pyrotechnics, 2012, 37, 12-23.
5. R. Wolffenstein, Berichte der deutschen chemischen Gesellschaft, 1895, 28, 2265-2269.
6. F. Dubnikova, R. Kosloff, J. Almog, Y. Zeiri, R. Boese, H. Itzhaky, A. Alt and E. Keinan, Journal of the American Chemical Society, 2005, 127, 1146-1159.
7. R. Schulte-Ladbeck and U. Karst, Analytica chimica acta, 2003, 482, 183-188.
8. S. Parajuli and W. Miao, Analytical chemistry, 2013, 85, 8008-8015.
9. C. L. Rhykerd, D. W. Hannum, D. W. Murray and J. E. Parmeter, National Contest Journal, 1999, 20531.
10. D. J. Williams, W. R. Creasy, R. A. Fry, V. L. Bevilacqua and H. D. Durst, Main Group Chemistry, 2010, 9, 309-314.
11. D. Jiang, L. Peng, M. Wen, Q. Zhou, C. Chen, X. Wang, W. Chen and H. Li, Analytical chemistry, 2016, 88, 4391-4399.
12. R. M. Burks and D. S. Hage, Analytical and bioanalytical chemistry, 2009, 395, 301-313.
13. A. Kende, F. Lebics, Z. Eke and K. Torkos, Microchimica acta, 2008, 163, 335-338.
14. K. L. Peters, I. Corbin, L. M. Kaufman, K. Zreibe, L. Blanes and B. R. McCord, Analytical Methods, 2015, 7, 63-70.
15. G. White, Journal of Forensic Sciences, 1992, 37, 652-656.
16. H. K. Evans, F. Tulleners, B. Sanchez and C. A. Rasmussen, Journal of forensic sciences, 1986, 31, 1119-1125.
17. S. Zitrin, S. Kraus and B. Glattstein, Year.
18. L. Widmer, S. Watson, K. Schlatter and A. Crowson, Analyst, 2002, 127, 1627-1632.
19. B. T. Fedoroff, *Encyclopedia of explosives and related items*, Picatinny Arsenal, 1960.

20. J. Yinon, *Forensic and environmental detection of explosives*, John Wiley & Sons, 1999.
21. A. J. Bellamy, Journal of Forensic Sciences, 1999, 44, 603-608.
22. A. Ž. Tomović, H. Miljkovic, M. S. Dražić, V. P. Jovanović and R. Zikic, Physical Chemistry Chemical Physics, 2023, 25, 26648-26658.
23. M. Maziejuk, M. Szyposzyńska, A. Spławska, M. Wiśnik-Sawka and M. Ceremuga, Sensors, 2021, 21, 4545.
24. F. Dubnikova, R. Kosloff, Y. Zeiri and Z. Karpas, The Journal of Physical Chemistry A, 2002, 106, 4951-4956.
25. L. Lazarowski, L. P. Waggoner, S. Krichbaum, M. Singletary, P. Haney, B. Rogers and C. Angle, Frontiers in Veterinary Science, 2020, 7, 597.
26. M. A. Walter, D. Pfeifer, W. Kraus, F. Emmerling, R. J. Schneider, U. Panne and M. G. Weller, Langmuir, 2010, 26, 15418-15423.
27. Q. Zhang, X. Zou, Q. Liang, H. Wang, C. Huang, C. Shen and Y. Chu, Journal of the American Society for Mass Spectrometry, 2018, 30, 501-508.
28. M. Amani, Y. Chu, K. L. Waterman, C. M. Hurley, M. J. Platek and O. J. Gregory, Sensors and Actuators B: Chemical, 2012, 162, 7-13.
29. E. Capua, R. Cao, C. N. Sukenik and R. Naaman, Sensors and Actuators B: Chemical, 2009, 140, 122-127.
30. S. Malashikhin and N. S. Finney, Journal of the American Chemical Society, 2008, 130, 12846-12847.
31. S. Fan, P. L. Burn and P. E. Shaw, RSC advances, 2019, 9, 7032-7042.
32. S. Fan, J. Lai, P. L. Burn and P. E. Shaw, ACS sensors, 2019, 4, 134-142.
33. M. E. Germain and M. J. Knapp, Inorganic chemistry, 2008, 47, 9748-9750.
34. Y. Li, X. Liu, G. Zhang, R. Wang, R. Yue, G. Liao, Z. Sun and Y. Liu, Journal of Chemical Research, 2022, 46, 17475198221117409.
35. S. K. Mamo and J. Gonzalez-Rodriguez, Sensors, 2014, 14, 23269-23282.
36. R. A. Munoz, D. Lu, A. Cagan and J. Wang, Analyst, 2007, 132, 560-565.
37. G. Xie, X. Lv, P. Zhang, B. Liu, L. Gao, J. Duan, B. Ma and Z. Wu, Nano Select, 2020, 1, 419-431.
38. S. H. Hosseini, S. Mousavi, A. Mazlomifar, A. Parsa and R. Tehrani, Available at SSRN 4105306.
39. S. Saglam, A. Uzer and R. Apak, Analytical Chemistry, 2022, 94, 17662-17669.
40. B. Gökdere, A. Üzer, S. Durmazel, E. Erçağ and R. Apak, Talanta, 2019, 202, 402-410.
41. G. Zhang, X. Zou, H. Li and Y. He, Analyst, 2021, 146, 6187-6192.
42. A. Üzer, S. Durmazel, E. Erçağ and R. Apak, Sensors and Actuators B: Chemical, 2017, 247, 98-107.
43. Z. Can, A. Uzer, K. Turkekul, E. Ercag and R. Apak, Analytical chemistry, 2015, 87, 9589-9594.
44. N. Bagheri, A. Khataee, J. Hassanzadeh and B. Habibi, Journal of Hazardous Materials, 2018, 360, 233-242.
45. J. García-Calvo, P. Calvo-Gredilla, M. Ibáñez-Llorente, D. C. Romero, J. V. Cuevas, G. García-Herbosa, M. Avella and T. Torroba, Journal of Materials Chemistry A, 2018, 6, 4416-4423.
46. R. Khadka, C. Carraher, C. Hamiaux, J. Travas-Sejdic and A. Kralicek, Biosensors and Bioelectronics, 2020, 153, 112040.
47. T. Wasilewski, J. Gębicki and W. Kamysz, TrAC Trends in Analytical Chemistry, 2021, 142, 116330.
48. T. Onodera and K. Toko, Sensors, 2014, 14, 16586-16616.
49. J. C. Oxley, J. L. Smith, J. Moran, K. Nelson and W. E. Utley, Year.
50. A. Stambouli, A. El Bouri, T. Bouayoun and M. Bellimam, Forensic Science International, 2004, 146, S191-S194.
51. P. Hehet, M. Pütz, B. Kämmerer, G. Umlauf, O. Geiss, J. G. N. Caetano, K. Karaghiosoff and M. Wende, Forensic Science International, 2023, 348, 111673.
52. I.Cotte-Rodrı´guez,H. Chen and R.G.Cooks, ChemComm, 2006, 953-955.
53. Y. M. Taha, M. T. Saowapon, and H. D. Osthoff, Analytical and Bioanalytical Chemistry ,2018, 410, 4203–4212
54. W. Fan, M. Young, J. Canino, J. Smith, J. Oxley and J. R. Almirall, Analytical and bioanalytical chemistry, 2012, 403, 401-408.
55. C. Schaefer, M. Lippmann, M. Beukers, N. Beijer, B. van de Kamp, J. Knotter and S. Zimmermann, Analytical Chemistry, 2023, 95, 17099-17107.
56. E. Almenar, A. M. Costero, P. Gavina, S. Gil and M. Parra, Royal Society Open Science, 2018, 5, 171787.
57. K. A. Vassell and J. H. Espenson, Inorganic Chemistry, 1994, 33, 5491-5498.
58. S. Yamazaki, Bulletin of the Chemical Society of Japan, 1996, 69, 2955-2959.
59. Y. An, X. Xu, K. Liu, X. An, C. Shang, G. Wang, T. Liu, H. Li, H. Peng and Y. Fang, Chemical Communications, 2019, 55, 941-944.
60. M. Al Kobaisi, S. V. Bhosale, K. Latham, A. M. Raynor and S. V. Bhosale, Chemical reviews, 2016, 116, 11685-11796.
61. J. Fan, X. Chang, M. He, C. Shang, G. Wang, S. Yin, H. Peng and Y. Fang, ACS applied materials & interfaces, 2016, 8, 18584-18592.
62. V. Marx, Nature methods, 2015, 12, 187-190.
63. J. B. Grimm, B. P. English, J. Chen, J. P. Slaughter, Z. Zhang, A. Revyakin, R. Patel, J. J. Macklin, D. Normanno and R. H. Singer, Nature methods, 2015, 12, 244-250.
64. X. Liu, Q. Qiao, W. Tian, W. Liu, J. Chen, M. J. Lang and Z. Xu, Journal of the American Chemical Society, 2016, 138, 6960-6963.
65. H. Liu, X. Xu, Z. Shi, K. Liu and Y. Fang, Analytical Chemistry, 2016, 88, 10167-10175.
66. X. Cheng, Z. Cai, J. Dong, J.Li, C. Zhao, J. Ma, Q. Zhou and Xincun Dou, Aggregate 2026, 7,e70294.
67. H. Lin and K. S. Suslick, Journal of the American Chemical Society, 2010, 132, 15519-15521.
68. D. Lu, A. Cagan, R. A. Munoz, T. Tangkuaram and J. Wang, Analyst, 2006, 131, 1279-1281.
69. E. Sella and D. Shabat, Chemical communications, 2008, 5701-5703.
70. A. W. Apblett, B. Kiran, S. Malka, N. F. Materer and A. Piquette, Ceramic Nanomaterials and Nanotechnologies IV, 2006, 172, 29-35.

71. I. T. Jolliffe, N. T. Trendafilov and M. Uddin, Journal of computational and Graphical Statistics, 2003, 12, 531-547.
72 J. C. Oxley, J. L. Smith, K. Shinde and J. Moran, Propellants, Explosives, Pyrotechnics: An International Journal Dealing with Scientific and Technological Aspects of Energetic Materials, 2005, 30, 127-130.
73. S. Zhang, X. Zhao, H. Niu, Y. Shi, Y. Cai and G. Jiang, Journal of hazardous materials, 2009, 167, 560-566.
74. Y. Wu, Y. Ma, G. Xu, F. Wei, Y. Ma, Q. Song, X. Wang, T. Tang, Y. Song and M. Shi, Sensors and Actuators B: Chemical, 2017, 249, 195-202.
75. B. Keskin Çekem, A. Üzer and R. Apak, Microchemical Journal, 2024, 207, 111853.
76. S. M. Tawfik, A. A. Abd-Elaal and Y.-I. Lee, Analyst, 2021, 146, 2894-2901.
77. A. R. Hill, M. Edgar, M. Chatzigeorgiou, J. C. Reynolds, P. F. Kelly and C. S. Creaser, European Journal of Mass Spectrometry, 2015, 21, 265-274.
78. R. S. Ray, B. Sarma, S. Mohanty and M. Misra, Talanta, 2014, 118, 304-311.
79. S. Wang, H. Chen, H. Xie, L. Wei, L. Xu, L. Zhang, W. Lan, C. Zhou, Y. She and H. Fu, Food Chemistry, 2021, 346, 128923.
80. M. Saqib, S. Bashir, S. A. Kitte, H. Li and Y. Jin, Chemical Communications, 2020, 56, 1827-1830
81. A. Revilla-Cuesta, I. Abajo-Cuadrado, M. Medrano, M. M. Salgado, M. Avella, M. T. Rodríguez, J. García-Calvo and T. Torroba, ACS Applied Materials & Interfaces, 2023, 15, 32024-32036.
82. Ö. K. Koç, A. Üzer and R. Apak, Applied Materials Today, 2025, 44, 102760.
83. Ö. K. Koç, A. Üzer and R. Apak, Talanta, 2026, 301, 129275.
84. I. Abajo-Cuadrado, A. Revilla-Cuesta, R. Fernández-Ordóñez, J. R. Santana-Tejada, Y. Moreno-Macías, C. Almeida-Estévez, C. Hernando-Muñoz, J. García-Calvo, M. Avella and T. Torroba, Sensors & Diagnostics, 2026, https://doi.org/10.1039/D5SD00218D.